DIFFUSION TENSOR IMAGING AND TRACTOGRAPHY IN EPILEPSY SURGERY CANDIDATES

Daniel Nilsson

GÖTEBORG UNIVERSITY

Institute of Neuroscience and Physiology
Epilepsy Research Group
Sahlgrenska Academy
2008

"*I have a monster in my head.*"

4-year old boy describes his daily seizures characterized by extreme fear.

DIFFUSION TENSOR IMAGING AND TRACTOGRAPHY IN EPILEPSY SURGERY CANDIDATES

Daniel Nilsson, Institute of Neuroscience and Physiology, Epilepsy Research Group, Sahlgrenska Academy at Göteborg University, Sweden

ABSTRACT

In selected patients with medically refractory epilepsy, surgical treatment can render the patients seizure free or significantly reduce seizure frequency. Temporal lobe resection (TLR) for temporal lobe epilepsy (TLE) is the most commonly performed epilepsy surgery procedure. A visual field defect (VFD) due to injury to the optic radiation (OR) may occur after TLR. Diffusion tensor imaging (DTI) evaluates the structural integrity of brain tissue by measuring water diffusion and provides information on the directionality and magnitude of diffusion motion. DTI can be used to assess the effects of seizures on the brain parenchyma and DTI-based tractography (TG) can visualize white matter tracts such as the OR non-invasively

First, we evaluated the frequency of VFD after TLR in 50 patients with TLE and investigated if the extent of lateral TLR correlated with the frequency of VFD. We found that quadrantanopia due to injury to the OR occurred in 50% of patients and there was no association between the extent of lateral resection and VFD. In a second study we used TG to assess the anatomical location of the OR and the interindividual variability in the anterior extent of the OR in seven normal controls and two patients with previous TLR. TG could depict the OR in all cases and demonstrated a considerable variability in the anterior extent of the OR. The mean distance from the temporal pole to the anterior edge of Meyer´s loop was 44 mm bilaterally (range 34-51 mm). TG demonstrated a disruption of the tract depicting Meyer´s loop in one patient with quadrantanopia. In a third study, we used DTI to evaluate the effects of seizures on the diffusion properties in temporal lobe and cingulate gyrus white matter in eight children with TLE. We found bilateral changes in the diffusion properties which may reflect effects of frequent seizures on the white matter. The presence of bilateral alterations in diffusivity precluded seizure lateralization. In a fourth study we used DTI and TG to quantitatively assess the structural integrity of white matter tracts adjacent to low-grade brain tumors causing seizures in 11 children. We found preserved structural integrity of the white matter as indicated by preserved DTI indices of the white matter adjacent to the tumor and also displacement of the white matter tracts adjacent to the tumor in 10/11 children.

TG provides a non-invasive means of evaluating the major white matter tracts. This is important for presurgical planning to improve and individualize the preoperative risk analysis and prevent neurological deficits. However, limitations of the technique must be considered before it is used routinely and prospective studies using TG to assess the OR in TLE patients before TLR are needed to determine its clinical value. DTI may contribute to the multimodal evaluation in medically refractory epilepsy with information on the effects of focal seizures on the brain. However, longitudinal studies are needed to clarify these effects in more detail and to decide if this information may be useful to guide selection of epilepsy surgery candidates.

Key words: epilepsy, epilepsy surgery, temporal lobe resection, optic radiation, diffusion tensor imaging, tractography

ORIGINAL PAPERS

This thesis is based on the following papers:

I. **Visual field defects after temporal lobectomy - comparing methods and analysing resection size**
Nilsson D, Malmgren K, Rydenhag B, Frisen L. *Acta Neurol Scand* 2004; 110(5):p 301-307

II. **Intersubject variability in the anterior extent of the optic radiation assessed by tractography**
Nilsson D, Starck G, Ljungberg M, Ribbelin S, Jönsson L, Malmgren K, Rydenhag B. *Epilepsy Res* 2007 Oct;77(1):11-6.

III. **Bilateral diffusion tensor abnormalities of temporal lobe and cingulate gyrus white matter in children with temporal lobe epilepsy**
Nilsson D, Go C, Rutka J T, Snead III. O C, Raybaud C R, Rydenhag B, Mobbitt D, Widjaja E.
Submitted

IV. **Preserved structural integrity of white matter adjacent to low-grade tumors**
Nilsson D, Rutka J T, Snead III. O C, Raybaud C R, Widjaja E.
Childs Nerv Syst 2008; 24(3): p 313-320

LIST OF ABBREVIATIONS:

ADC	Apparent diffusion coefficient
ATL	Anterior temporal lobe resection
CGWM	Cingulate gyrus white matter
DNET	Dysembryoplastic neuroepithelial tumor
DTI	Diffusion tensor imaging
EEG	Electroencephalography
FA	Fractional anisotropy
FACT	Fibre assignment by continuous tracking
FLAIR	Fluid attenuated inversion recovery
FMT	Fast marching tractography
ILAE	International League Against Epilepsy
MATL	Modified anterior temporal lobe resection
MCD	Malformations of cortical development
MD	Mean diffusivity
MEG	Magnetoencephalography
MNI	Montreal Neurological Institute
MRI	Magnetic resonance imaging
MTS	Mesial temporal sclerosis
OR	Optic radiation
PICO	Probabilistic index of connectivity
ROI	Region of interest
SAHE	Selective amygdalohippocampectomy
TG	Tractography
TLE	Temporal lobe epilepsy
TLR	Temporal lobe resection
VFD	Visual field defect
TLWM	Temporal lobe white matter
VOI	Volume of interest
Voxel	Smallest volume element used in three-dimensional imaging

$\lambda_{\parallel}$ = parallel diffusivity = λmajor = primary eigenvalue
$\lambda_{\perp}$ = perpendicular diffusivity = (λmedium + λminor)/2
λmajor = primary eigenvalue
λmedium = secondary eigenvalue
λminor = tertiary eigenvalue

CONTENTS

1. INTRODUCTION AND BACKGROUND

Epilepsy is one of the most common neurological disorders with a prevalence of 0.5-1% in the general population [1-3]. Epilepsy is a brain disorder characterized by repeatedly occurring (more than two) spontaneous seizures even though this definition is currently under discussion [4]. All seizures are clinical manifestations of abnormal and excessive discharges of groups of neurons in the brain. The characteristics of a seizure depend on the brain regions involved, including the region of onset as well as the subsequent spread of the discharge. As a consequence the variety of seizure manifestations is immense, including motor, sensory (olfactory, visual and auditory), autonomic or psychic events. The seizures can be either partial with a focal onset, or generalized, without clear anatomical localisation or with evidence of bilateral onset. If alterations in the level of consciousness occur in a partial seizure it is called complex, in contrast to simple seizures where the patient is alert and responsive.

Most seizures have an abrupt onset, causing a loss of control, making epilepsy a major handicap. Even though many types of epilepsy can be controlled by antiepileptic drugs, patients with medically refractory epilepsy suffer socially and psychologically, in addition to having a considerably increased mortality rate [5-8]. Some of these patients, after careful selection, will benefit from epilepsy surgery, with improvements in both seizure frequency and quality of life [9, 10].

In the assessment of epilepsy surgery candidates, magnetic resonance imaging (MRI) is an important tool to detect potentially epileptogenic lesions as well as their anatomical relationship to important functional areas of the brain. Diffusion tensor imaging (DTI) is an advanced MRI technique which can indirectly evaluate the structural integrity of brain tissue by measuring water diffusion and its directionality in three dimensions [11]. DTI has the potential to localize subtle epileptogenic lesions not seen on conventional MRI. In addition, information on the structural properties of brain tissue, provided by DTI, may give important insights into the pathophysiology of epilepsy and the acute and chronic effects of seizures on the brain. Tractography is a technique based on DTI data that visualizes white matter tracts in vivo, information that may be used to avoid surgical injury to functionally important white matter tracts. This thesis is focused on the applications and limitations of DTI and tractography in the preoperative work-up for epilepsy surgery. The findings of these studies could improve preoperative risk counselling, prevent injury to white matter tracts in epilepsy surgery candidates and increase understanding of the effects of seizures on the brain.

1.1 MEDICALLY REFRACTORY EPILEPSY

1.1.1 Definition and epidemiology

Pharmacological treatment is the first choice of treatment in both adults and children with epilepsy. This treatment is however symptomatic, preventing seizures from occurring, but does not treat the underlying cause of the epilepsy. Approximately two-thirds of patients with epilepsy become seizure-free on established antiepileptic drug treatment [12]. Thus about one-third of patients diagnosed with epilepsy develop what may be referred to as

"medically refractory epilepsy". In this group many different etiologies are found, including inflammatory or infectious conditions, malformations of cortical development, low-grade tumors, arteriovenous malformations, genetic syndromes and hippocampal sclerosis. However, in up to 30 % of these patients, a structural cause of the epilepsy can not be found, even if optimal neuroimaging techniques are used.

The definition of "medically refractory epilepsy" is not entirely clear. However, an often used recommendation is to investigate epilepsy surgery as an option in patients with focal epilepsy when two different drug treatments have failed and after a sufficient period of time has passed (usually 2 years, less in children) [5]. Unfortunately it is common that patients are tried on additional drugs and withheld from evaluation for epilepsy surgery even though the chances of seizure control with the third or fourth antiepileptic drug are low [5]. The average duration of medically refractory epilepsy prior to surgery in adults is of the order of 20 years [13, 14]. This may cause unnecessary suffering and increased mortality as patients with medically refractory epilepsy have a significantly increased risk of sudden death [7, 8, 15]. Hence, patients with epilepsy refractory to medical treatment should be promptly referred to a specialized epilepsy centre where different treatment options, including epilepsy surgery, can be addressed.

1.1.2 Definition of temporal lobe epilepsy

Temporal lobe resection (TLR) for temporal lobe epilepsy (TLE) is the most common epilepsy surgery procedure, comprising more than 70% of procedures in adult epilepsy surgery patients and around 50% of procedures performed in children [16]. TLE is thus the most important surgically treatable epilepsy. There are two main types of TLE, depending on the anatomical structures involved: i) mesial TLE involving the medial temporal lobe, including the hippocampus and amygdala, and ii) lateral or neocortical TLE [9]. Mesial TLE is the most common type and the seizure manifestations are typically complex partial seizures starting with a characteristic aura such as fear, anxiety or epigastric rising sensation followed by movement arrest, alteration of consciousness, and automatisms.

In children below 6 years of age seizure manifestations in TLE can be atypical, and include bilateral motor activation, head nodding as well as hypermotor postures [17-19]. The limitations in defining a subjective experience in pre-school children, where only changes in facial expression may suggest an emotional reaction, make the clinical diagnosis of temporal lobe seizures more difficult in these patients [19]. However after 7 years of age, children with TLE tend to have seizures similar to those seen in adult patients [18, 20]. Depending on seizure spread and seizure duration, positive ictal motor symptoms and marked postictal confusion might be found. After a seizure there is usually a post-ictal dysfunction, most frequently cognitive impairment, memory deficits, mood changes, and language deficits [17].

1.1.3 Causes of temporal lobe epilepsy in children and adults

The pathophysiological mechanism causing TLE is in most cases unknown. In adults, mesial temporal sclerosis (MTS) is found in over 70% of patients who had temporal lobe surgery for mesial TLE [21-24]. The most prominent histopathological abnormalities in MTS include selective cell loss with secondary astroglial proliferation in layer CA1, CA3 and CA4 of the hippocampus [25-27], but changes in the amygdala, uncus and parahippocampal gyrus may also be present [28]. If the cell loss is pronounced, it has a characteristic appearance on imaging, displaying bright signal on T2 and FLAIR images and commonly volume loss (Fig 1) [29-32]. Even though MTS in TLE has been thought to be localized to the medial temporal lobe, autopsy studies as well as diffusion tensor imaging studies suggest that the pathological changes may extend well outside the temporal lobe [33-38]. The nature of these changes is not clear and they may either be a consequence of frequent seizures or reflect a generalized disorder that predisposes the brain to react with seizures.

Whether MTS is the cause of TLE or a consequence of frequent seizure activity or possibly both cause and effect, has been debated [39, 40]. Serial MRI studies showing hippocampal atrophy in patients in limbic status epilepticus have shown that frequent seizures can cause MTS [30, 41]. Other, less common histopathological findings in adults with TLE are malformations of cortical development (MCD), ganglioglioma, low-grade astrocytoma, gliosis, cavernoma and vascular malformations [14, 42]. MTS may coexist with other pathological findings such as gliosis or a dysplasia, so called “dual pathology”. The frequency of this finding after TLR however varies widely between different studies, from 8% [43] to 79% [31] in children and from 15% [44] to 48% [21] in adults. These variations in frequency may be due to differences in the analysis of the histological specimens and classification of the findings.

In children with TLE the histopathological spectrum differs from what is seen in adults. Developmental anomalies such as cortical malformations or dysplasias and low-grade tumors are seen much more frequently whereas MTS only occurred in 13 % of children having TLR for TLE in a recent study [43]. Epilepsy in children is also different from adults as the seizure activity affects the developing brain. Lesions causing epilepsy may interfere with the development of the brain, both by occupying space, forcing brain functions to move to unusual brain regions, and by disturbing normal brain development with frequent seizure activity, causing developmental delay and/or behavioural problems [45-47]. A significant proportion of children with TLE are refractory to medical treatment, and these children are important to identify. To prevent the possibly disastrous effects of epilepsy on the developing brain, children with medically refractory epilepsy should be identified without delay, without waiting for a specified period, and referred to a centre with expertise in pediatric epilepsy surgery for evaluation [46].

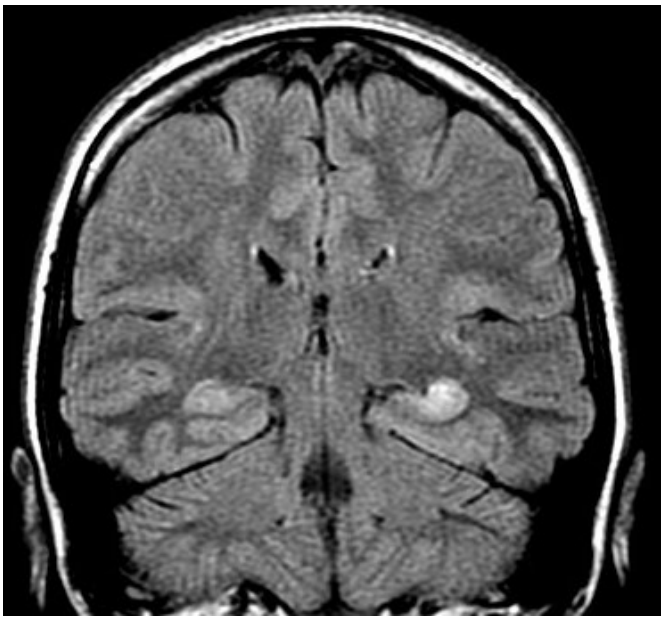

Fig 1. *Coronal FLAIR image showing an increased signal in the left hippocampus, in keeping with mesial temporal sclerosis*

1.1.4 Developmental brain tumors as a cause of epilepsy

Certain slow-growing, benign brain tumors such as dysembryoplastic neuroepithelial tumor (DNET), ganglioglioma and pleomorphic xanthoastrocytoma frequently present with seizures [48]. These tumors are one of the most common causes of medically refractory seizures in children [49], but are also seen in adult patients with focal epilepsy [14, 42]. Excision of the lesion together with the epileptogenic zone, which may extend to the surrounding brain region, usually results in excellent seizure control with 75% of patients in Engel class I or II[1] after resection of DNET:s and over 90 % of patients in Engel class I or II after resection of gangliogliomas in children [43]. Resection of these tumors has a favourable seizure outcome also in adults [50]. If the epilepsy can be controlled medically, a conservative management strategy may be warranted, however follow-up imaging is mandatory as there is a small risk of malignant transformation, and the risk of having epilepsy, including delayed development and drug-related side effects, must also be carefully weighed against the risk of surgery.

Surgery for supratentorial low-grade tumors can be challenging as they frequently are situated close to functionally critical cortex and/or white matter tracts and because the patients rarely have any preoperative neurological deficit. DTI and tractography could potentially be used to delineate and determine the structural integrity of the white matter

[1] (Engel Class I = seizure freedom, with or without aura; Class II = rare disabling seizures or nocturnal seizures only)

tracts adjacent to low-grade tumors. This information may improve preoperative counselling regarding risk of operative injury and reduce the risk of a neurological deficit after surgery.

1.2 SURGICAL TREATMENT OF MEDICALLY REFRACTORY EPILEPSY

At the end of the nineteenth century John Hughlings Jackson reported that certain brain regions were associated with specific seizure characteristics [51]. Based on Jackson´s findings the first successful surgical procedures for epilepsy were performed by Victor Horsley in London at the end of the 19th century [52]. The areas to be resected were determined by careful neurological examination and observation of the seizures. With the discovery of electroencephalography (EEG) in 1929 the seizure onset could be localized more accurately. This led to a renewal of the interest in epilepsy surgery and by 1950 over 70 TLR had been performed by Wilder Penfield at the Montreal Neurological Institute, using only clinical and neurophysiological localisation of the epilepsy [53]. The advent of video-EEG monitoring and modern neuroimaging, most notably high-resolution MRI, has greatly facilitated the localization of epileptogenic lesions [54]. Today, epilepsy surgery is an established treatment for medically refractory epilepsy with proven benefit in terms of seizure outcome and improved quality of life [55].

1.2.1 Preoperative evaluation for epilepsy surgery

In both adults and children, the preoperative evaluation for epilepsy surgery aims at identifying the cortical area crucial for seizure production, i.e. the epileptogenic zone. The preoperative investigation must also identify functionally important brain regions surrounding the epileptogenic zone which should be avoided in a resection. Neuroimaging techniques such as functional MRI or motor field mapping using magnetencephalography (MEG) can provide important information on the localization of cortical areas responsible for motor, sensory and language function non-invasively. The base-line evaluation for epilepsy surgery includes clinical examination, structural MRI, video-EEG with surface electrodes and neuropsychological assessment [9].

The findings from the base-line work-up are used to evaluate whether there is concordance of findings with a single surgically amenable seizure focus, and to estimate the risk of a postoperative functional deficit. If the findings are consistent with a single seizure focus which is surgically resectable without major risks of postoperative deficits, the patient is offered surgery. This is the case in most adults with TLE, where the base-line work-up is frequently sufficient to offer the patient TLR [56]. In case of discordant findings, or if there is a significant risk of injury to functionally important cortex, either the patient may not be considered as a good candidate for epilepsy surgery or additional investigations may be required. Depending on the situation, additional investigations may include repeated neuroimaging, including functional MRI, ictal and interictal single photon emission CT (SPECT), MEG, invasive EEG monitoring using subdural and/or depth electrodes and/or a Wada test. Invasive video-EEG monitoring has two primary goals: i) to more accurately define the epileptogenic zone and ii) to identify functionally important cortex such as motor, sensory and language areas by direct cortical stimulation. This can be particularly important in children with developmental lesions, where cortical areas may be atypically located. After evaluation of the additional information, an

analysis of the potential benefits and risks of epilepsy surgery for the individual patient determines whether the patient will be recommended epilepsy surgery or not.

1.2.2 Procedures used in epilepsy surgery

Two main types of procedures can be identified: i) resective procedures, aiming at removing the seizure-producing brain region, and ii) disconnective procedures, where the seizure focus cannot be removed, but by disrupting its connections the spread of seizures to adjacent brain regions can be limited or abolished. The resective procedures include TLR, extratemporal resection, lesionectomies including resection of the surrounding epileptogenic zone which can involve any of the frontal, parietal, occipital lobes or the insula and hemispherectomy/hemispherotomy. The main disconnective procedure is callosotomy but disconnection of hypothalamic hamartoma and subpial transsection to control seizure propagation also belong to this group. Vagal nerve stimulation, aiming at reducing the seizure frequency, can be used as a palliative approach when none of the other procedures mentioned are feasible.

1.2.3 Techniques used for temporal lobe resection

The aim of surgery for medically refractory TLE is to resect the epileptogenic zone, i.e. the hippocampus, parahippocampal gyrus, amygdala and sometimes parts of the lateral temporal lobe with a minimum of neurological deficit. Three types of resections dominate in reports from epilepsy surgery centres: classical anterior temporal lobe resection (ATL), modified anterior temporal lobe resection (MATL) and amygdalohippocampectomy (transsylvian or transcortical). ATL includes a large resection of the lateral temporal lobe, 4-6 cm:s from the temporal pole on the dominant side and 5-7 cm:s on the non-dominant side. The resection of the medial structures are not carried far posteriorly thus sparing the posterior hippocampus. Spencer modified the ATL with a smaller lateral resection, 4.5 cm:s behind the temporal pole regardless of the side and a larger medial extension reaching further posterior with the hippocampal resection [57] (Fig 4, 14). The advantage is less damage to the lateral temporal lobe structures and more resection of the medial epileptogenic structures. To be even more selective and only remove the medial temporal lobe structures Yasargil and Wieser developed the selective amygdalohippocampectomy (SAHE) performed through a transsylvian approach [58]. In this procedure the lateral temporal cortex is not resected, possibly reducing the risk of cognitive impairment postoperatively [59]. However this technique is more technically demanding and may have an increased risk of vascular injury [60]. SAHE may also have a less favourable seizure outcome in children with TLE, and is rarely used in children [50, 61]. All techniques described above require the identification and opening of the temporal horn of the lateral ventricle to resect the medial temporal lobe structures.

1.2.4 Seizure outcome after epilepsy surgery

Reports of seizure outcome after epilepsy surgery are often difficult to interpret as they tend to use different ways to report the results. Outcome is also related to the goals of surgery in the individual patient. For example a 50 % seizure reduction may be a major improvement in one patient, abolishing a debilitating type of seizure, whereas it can be a failure in another patient if incapacitating seizures persist. The only randomized

prospective study of outcome after epilepsy surgery has shown that more than 60% of the patients were seizure-free and another 15 to 20 % had a significant reduction in their seizure frequency following TLR [55]. A recent long-term follow-up has confirmed that the seizure outcome is consistent also ten years after TLR [62]. In children seizure outcome after TLR for TLE seems to be even better with up to 90 % of patients seizure-free, even though randomized controlled studies are lacking to confirm this [42, 43, 61, 63, 64]. The seizure outcome is similar for ATL, MATL and selective SAHE for adults, whereas in children SAHE may have a less favourable outcome [50, 61].

In extratemporal resective procedures the proportion of seizure-free patients is somewhat lower [63, 64]. Hemisperectomy/hemispherotomy has very good seizure outcome with more than 85 % in Engel Class I or II reported in two large studies [65, 66]. Callosotomy on the other hand, rarely results in seizure freedom, but can be an important palliative procedure by eliminating drop attacks [67]. Epilepsy surgery procedures in general carry a 2 % risk for major, unexpected complications [17, 68]. Minor complications, resolved within three months, occur in about 4-6% [68]. In modern series the mortality is well below 1% [68, 69].

1.2.5 Visual field defects after temporal lobe resection

In 1922 Harvey Cushing reported that damage to the optic radiation in the anterior temporal lobe produces a superior homonymous visual field defect (VFD) [70]. Later studies have confirmed that VFD is a common postoperative neurological deficit, occurring in 50-90 % of patients after TLR [71-77]. The VFD caused by TLR is typically a contralateral upper quadrantanopia with a horizontal lower border (Fig 9). The VFD usually spares the central-most visual field, due to the retinotopic organisation of the optic radiation, however, with larger resections the risk of central involvement may increase [78]. As a VFD is an expected deficit it is usually not regarded as a complication. Most patients do not notice the VFD, however in a study from the United Kingdom, 13 % of patients with a VFD following TLR were found to be ineligible to drive, despite being seizure-free [79].

1.2.6 Surgical anatomy of the optic radiation

The optic radiation, or geniculocalcarine tract, begins in the dorsal aspect of the lateral geniculate nucleus and projects to the primary visual cortex. After exiting the lateral geniculate nucleus, these myelinated fibres course anteriorly and laterally, sweeping over the temporal horn of the lateral ventricle before turning posteriorly, following the ventricular wall and finally turning medially, connecting to the visual cortex around the calcarine fissure. The optic radiation has a retinotopic organisation with an upper, a central and a lower bundle. The lower bundle mediates information from the homonymous inferior retinal quadrants corresponding to the contralateral superior visual field. This bundle forms the Meyer-Archambault loop first identified as a part of the optic radiation in 1906 by Archambault and later described in more detail by Meyer in 1907 [80, 81]. The central bundle mediates visual input from the retinal macula and is situated more posteriorly than the lower bundle and spreads out in the anterior-posterior direction. The upper bundle is even more posterior and mediates information from the contralateral inferior visual field and projects from the lateral geniculate body directly posteriorly to

the visual cortex [82, 83]. Barton et al have proposed a revised retinotopic model where the most anterior fibres of Meyer's loop represent the superior field, not the vertical meridian as previously thought [78].

Dissection of white matter in formalin-fixed brains gives a unique three-dimensional view of the anatomy of the optic radiation [84] (Fig 2). However, this technique can only be used ex vivo, and does not reliably separate one fibre system from another. In addition, the dissection of one white matter tract may lead to destruction of other tracts. To overcome these limitations, combinations of dissection techniques, staining techniques for white matter and MRI to separate the optic radiation from other fibre tracts in the temporal lobe such as the uncinate fasciculus and the inferior longitudinal fasciculus have been used [85-87]. Still, the exact location of Meyer´s loop in relation to the temporal horn of the lateral ventricle remains a controversy. To be able to spare the optic radiation in TLR or at least estimate the risk of causing a VFD as a result of surgery, the anatomical location of the optic radiation in the individual patient needs to be clarified.

Fig 2. *The dissected optic radiation on the left side seen from below, left on the picture is anterior. After leaving the lateral geniculate nucleus (CGL), the optic radiation courses anterolaterally, forming Meyer´s loop (ML). Then it continues posteriorly, to the visual cortex (VC). Reprinted from [84] with permission from S Karger, Basel .*

1.3 PRINCIPLES OF DIFFUSION TENSOR IMAGING AND TRACTOGRAPHY

1.3.1 Diffusion tensor imaging

Diffusion tensor imaging (DTI) is a MRI technique that can indirectly evaluate the integrity of white matter by measuring water diffusion and its directionality in three dimensions [11]. From information about the direction of diffusion in at least six different non-parallel directions, the diffusion tensor can be calculated and is often represented three-dimensionally as a diffusion ellipsoid [11] (Fig 3). The fractional anisotropy (FA) and the major, medium and minor eigenvalues (λmajor, λmedium, λminor), can be derived from this [11]. FA is a rotationally invariant parameter that represents the ratio of the anisotropic component of the diffusion tensor to the whole diffusion tensor [11]. FA values range from 0 to 1, where 0 represents maximal isotropic diffusion as in a perfect sphere and 1 represent maximal anisotropic diffusion as in an infinitely elongated ellipsoid. The major, medium and minor eigenvalues specify the rates of diffusion along each of the three orthogonal axes of the diffusion ellipsoid. Diffusivity is frequently expressed as trace = λmajor + λmedium + λminor, or mean diffusivity, MD = trace/3. Trace and MD both provide an overall evaluation of the magnitude of diffusional motion in a three-dimensional volume element (voxel) or region.

FA and the direction of λmajor are commonly presented as a colour-coded fractional anisotropy map, where intensity represents the fractional anisotropy value and colour the direction of λmajor in each voxel (Fig 3). FA and MD are the most commonly used parameters for the diffusion properties of brain tissue. Both diffusivity and anisotropy vary widely between different brain regions in the normal brain (Fig 3). This heterogeneity reflects a variation in many factors, including the concentration of cellular macromolecules, cellular organization, cell density and the degree of myelination [88]. For example, as diffusion has a greater magnitude in parallel with axons, than perpendicular to axons, diffusion has a high anisotropy in regions with densely packed axons such as white matter [88]. Thus the diffusion characteristics of a tissue provide information on its structural properties.

To quantitatively analyze DTI data, either a voxel-based or a region of interest (ROI)-based approach is used. The former is a statistical comparison voxel by voxel, usually between patients and controls, and requires that all brains are transformed into a common space such as the Talairach or MNI space [89]. To achieve this, a process called normalization is necessary to reduce the overall variability between sizes and shapes between brains. Even though this is a statistically rigorous methodology, which assesses the whole brain, the normalization required may cause distortions resulting in reduced sensitivity and/or geometric distortions, particularly in children with brain malformations [90]. In the ROI-based approach a region is outlined manually and the diffusion parameters within the ROI is measured. The main limitation of this approach is its user-dependency which may result in a relatively large interobserver variability. To reduce interobserver variability, a ROI can be used as a seed point for tractography with a threshold for FA applied, and the resulting volume, formed by a large number of voxels, can be used for the calculation. This technique can also be used to quantitatively assess the diffusion properties of specific white matter tracts.

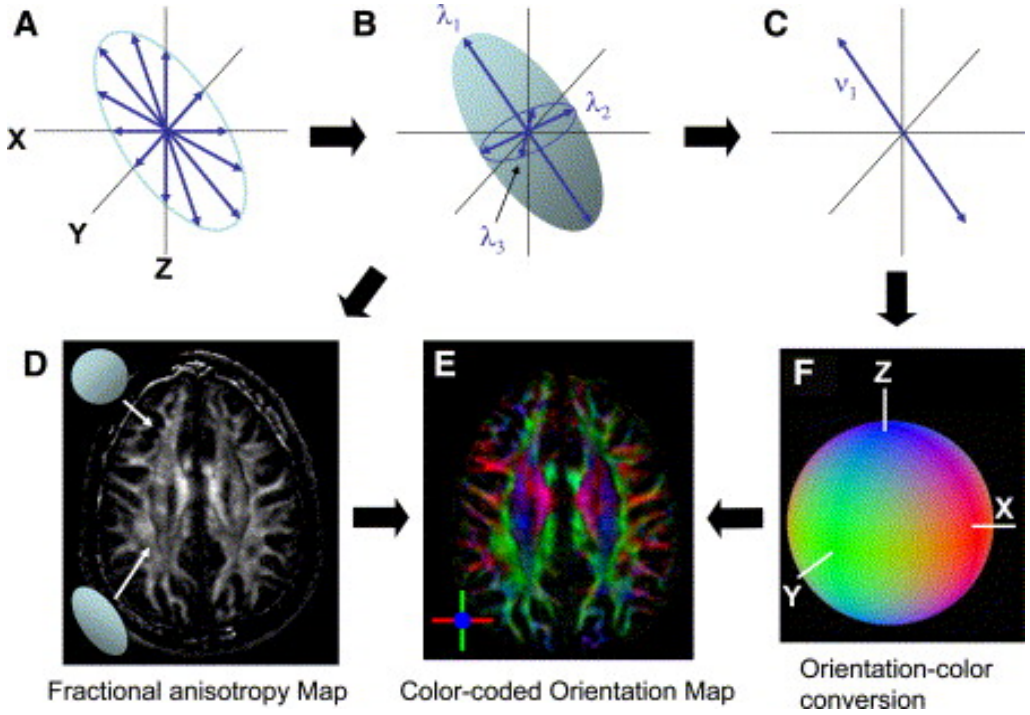

Fig 3. *The principle of DTI. A: Diffusion is measured along multiple axes. B: The shape of the "diffusion ellipsoid". C: The orientation of the longest axis in the ellipsoid, λ_{1} or λ_{major} is found. D: An anisotropy map is created where areas with low anisotropy are dark and areas with high anisotropy are bright. E: Color-coded anisotropy map with both the degree of anisotropy and the direction of the main vector, λmajor is represented. F: the color code is blue: cranio-caudal, red right-left and green anterior-posterior. Reproduced from [91] with permission.*

1.3.2 Tractography

Tractography is based on data from DTI and is the only available non-invasive technique which can delineate white matter tracts in vivo. The directional anisotropy information in each voxel provided by DTI is used to generate virtual maps of the white matter tracts. This is based on algorithms that determine how the voxels should be connected according to their anisotropy and direction. These algorithms can be placed in two broad categories: line propagation techniques and energy minimization techniques. Line propagation is based on algorithms that use local tensor information for each step of the propagation [92-94]. From a seed ROI the tracking follows the largest tensor in each voxel and connects them according to specific thresholds for the minimum FA and the maximal change of directions between two voxels. The FACT (fibre assignment by continuous tracking) algorithm is the most widely used in this group. The approach based on global energy minimization aims to find the energetically most favorable path between two voxels. The probability of connections between voxels is calculated, and from a seed point a volume of connected voxels can be calculated [95]. The most widely used techniques in this group are the FMT (fast marching tractography) and PICO (probabilistic index of connectivity).

In both approaches a "region of interest" i.e. a starting point for the calculation, and some type of threshold conditions (FA or number of iterations) under which the tracking is stopped are chosen manually. A development of the line propagation techniques allows several regions of interest to be chosen to "dissect" the fibres of interest from other fibres [93, 96]. This dissection method is knowledge-based and requires detailed understanding of the white matter anatomy, which makes it more user-dependent than the FMT or PICO techniques.

1.3.3 Limitations of diffusion tensor imaging and tractography

DTI and tractography have several limitations, which if not considered may have serious consequences for the interpretation of the information derived from these techniques [93, 97]. The voxel size used in diffusion tensor imaging is usually 1-15 mm^3. As an axon is in the order of 0.01 mm, the signal from one voxel represents thousands of axons which may have different directions. Artifacts due to subject motion, eddy currents, magnetic susceptibility or image noise can lead to a degraded or changed signal or geometric image distortions of the DTI data [97].

Tractography algorithms based on finding a single diffusion ellipsoid have difficulties tracking fibres that are crossing within a voxel [93]. The manual steps required to select regions of interest (ROI) and FA thresholds for termination of tractography involved in the line propagation techniques introduce a degree of subjectivity, which may affect reproducibility of the results. The direction of neural signal propagation within a white matter tract cannot be judged from the direction of water diffusion. Tractography results may also be affected by changed diffusion properties in white matter adjacent to lesions [98]. To define optimal conditions for tractography, the effects of different lesions on the diffusion properties of white matter tracts need to be studied.

Validation of tractography has mostly been qualitative, by comparing tractography to normal white matter anatomy derived from white matter dissections or histological studies [99, 100]. Some studies have compared tractography directly to invasive tracing techniques, such as manganese-enhanced MRI [101] and dextran amine tracing [102] with good correlation between methods, even though areas with crossing fibres or small tracts were not always accurately reproduced by tractography. Before tractography is used for presurgical planning, possible sources of error must be taken into consideration.

1.4 Applications of DTI and tractography in epilepsy surgery

DTI has the potential to identify epileptogenic lesions not seen on conventional MRI. [103]. Rugg-Gunn and co-workers have examined patients with focal epilepsy and negative MR and found an increased MD or FA in 10/30 patients, and in eight of these 10 patients, the lesions were concordant with EEG findings [104]. In a study of 22 patients with epilepsy and malformations of cortical development, reduced FA was found in 17/22 patients and increased MD in 10/22 patients [105]. These areas were within lesions seen on conventional imaging. In addition, areas of abnormal diffusion were found outside the cortical malformation with reduced FA in six patients and increased MD in nine. A good anatomical correlation has been reported between foci of increased ADC

and EEG abnormality recorded by depth electrodes in 7/16 patients with extratemporal focal cryptogenic epilepsy [106]. Together, these studies suggest that DTI is more sensitive than conventional MRI to detect subtle lesions. Therefore, in cases where optimal conventional MRI can not identify a lesion, quantitative DTI analysis may be of value. However, due to its low specificity, the information from DTI must be assessed as part of the multimodal evaluation of epilepsy surgery candidates [103].

DTI may also detect functional or structural changes secondary to involvement in the epileptic network, and could potentially visualize this network. In TLE the epileptogenic zone has been suggested to be involved in a hyperexcitable network with extensive connections between the mesial temporal lobe structures and the thalamus, limbic structures and the lateral temporal lobe [107]. Studies in adult TLE patients suggest that white matter structure and/or function surrounding the epileptogenic zone is altered, possibly reflecting involvement in an epileptic network [35, 108, 109]. The changes in white matter diffusion properties seen in adult TLE patients raise the question if these changes are present also in pediatric TLE patients. Such information may increase our understanding of the effects of seizures on the brain and contribute to the presurgical evaluation of children with TLE.

Tractography has been widely used to delineate normal white matter anatomy [94, 96]. Several studies have reported on the potential of preoperative tractography to visualize white matter tracts prior to neurosurgical resection. Typically, tractography has been used to visualize the relation between tumor and corticospinal tract prior to or during resection [110-115]. Tractography may also be useful prior to epilepsy surgery to visualize white matter tracts and their relationship to epileptogenic lesions. Tractography of the optic radiation is feasible [82] and some studies suggest that injury to white matter tracts seen on tractography correlates to neurological deficit [116, 117]. To provide information on the intersubject variability in the anatomical position and anterior extent of Meyer´s loop, and to determine whether tractography may be of value to prevent visual field deficits, further studies are necessary.

1.5 AIMS OF THE STUDY

Epilepsy surgery is an excellent treatment for medically refractory epilepsy in selected patients. DTI is a neuroimaging technique providing information on the diffusion properties of white matter. This information may be used to localize subtle epileptogenic lesions in epilepsy surgery candidates and to improve understanding of the effects of acute and chronic seizures on the brain. In addition, DTI data can be used to generate maps of white matter tracts in vivo, tractography. This information may be used to reduce the risk of injury to functionally important white matter tracts in epilepsy surgery.

The aims of this study were the following:

-To describe the frequency of visual field defects after temporal lobe resection in the Göteborg epilepsy surgery series from 1987 to 1999

-To investigate if larger lateral temporal lobe resections result in a higher frequency of visual field defects than more limited resections

- To assess the interindividual variability in the anterior extent of Meyer´s loop by tractography

-To investigate if interictal diffusion properties in the temporal lobe and cingulate gyrus white matter are abnormal in children with TLE

-To assess the structural integrity of white matter tracts adjacent to supratentorial low-grade brain tumors in children with epilepsy by DTI and tractography

2. SUBJECTS AND METHODS

2.1 STUDY I

All epilepsy surgery patients in Göteborg are prospectively included in a research database. In the first part of this study, patients who had undergone TLR for pharmacoresistant TLE in the Göteborg Neurosurgical Department between 1987 and 1999, who had a normal preoperative perimetry and a follow-up perimetry performed 3 months after surgery were included. Fifty patients met these criteria, 27 were female and 23 were male and their mean age was 35.9 years. In the second part of the study only patients who had pre- and post-operative MRI available were included, leaving 34 patients for the analysis. The mean age in this group was 35.0 years and, there were 16 females and 18 males. Data on seizure outcome was collected two years after surgery and classified as seizure-free (including patients with aura only), ≥75 % seizure reduction and < 75% seizure reduction. Two different types of TLR were used during these 12 years, and after reviewing the patient charts, the patients were divided into anterior temporal lobe resection (ATL) or modified ATL (MATL) groups (see above).

Neuro-ophthalmological examination

Visual acuity, eye motility, pupillary reaction, full visual field examination by manual kinetic perimetry using a Haag–Streit Goldmann instrument and funduscopy were assessed by clinical neuro-ophthalmologists. VFDs were classed as less than a quadrant (<q), quadrantic (q), more than a quadrant (>q) or hemianopia (h).

Radiological studies of size of resection

As the studies were made in five different MRI units and study protocols, including slice thickness and coronal slice angle, varied widely between studies a method that could be used in this heterogeneous material had to be chosen. On post-operative T1-weighted MRI scans three coronal slices through the temporal lobe were selected (fig 4). The first coronal slice was through the optic chiasm (slice 1), in its central part if it was visible on several slices. The second was the most anterior slice containing the pontomesencephalic junction (slice 2). The third slice selected was the most anterior slice containing the fourth ventricle (slice 3). The distance from the temporal pole to slices 1, 2 and 3 was approximately 18, 36, and 58 mm, respectively, when the slices were identified in an MRI atlas with information derived from 152 T1-weighted stereotactic volumes in healthy subjects [89]. To further define the resected parts of the temporal lobe, four compartments of the lateral temporal lobe, the superior, median, inferior and hippocampal compartments were identified on each slice (Fig 5). The superior compartment contained the superior temporal gyrus, the median compartment the middle temporal gyrus, the inferior compartment the inferior temporal gyrus in slice 1 and also the fusiform gyrus in slices 2 and 3. The hippocampal compartment contained the uncus and parahippocampal gyrus in slice 1, and in slices 2 and 3 the hippocampus and the parahippocampal gyrus [118].

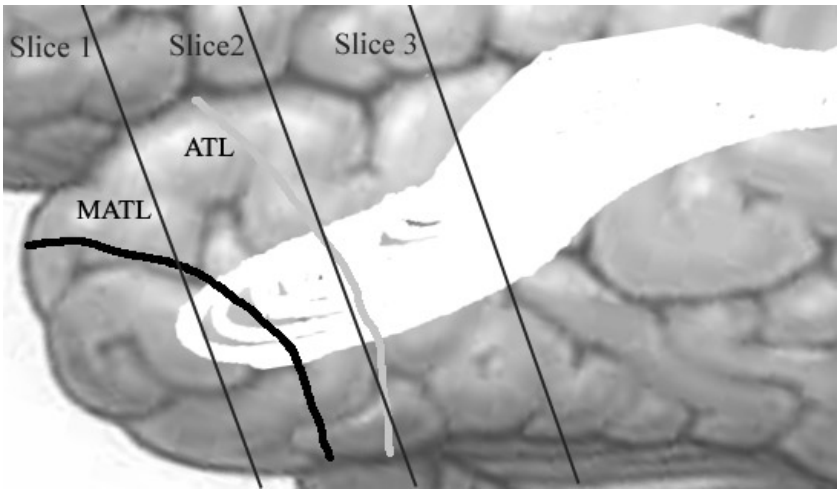

Fig 4. *The lateral temporal lobe with the approximate course of the optic radiation outlined in left lateral view. The approximate posterior resection line for a modified anterior temporal lobe resection (MATL) and a traditional ATL is marked. The estimated positions for the three selected slices (Slice1, 2, 3) of the temporal lobe are marked. The course of the optic radiation is modified from [119]. Reprinted with permission.*

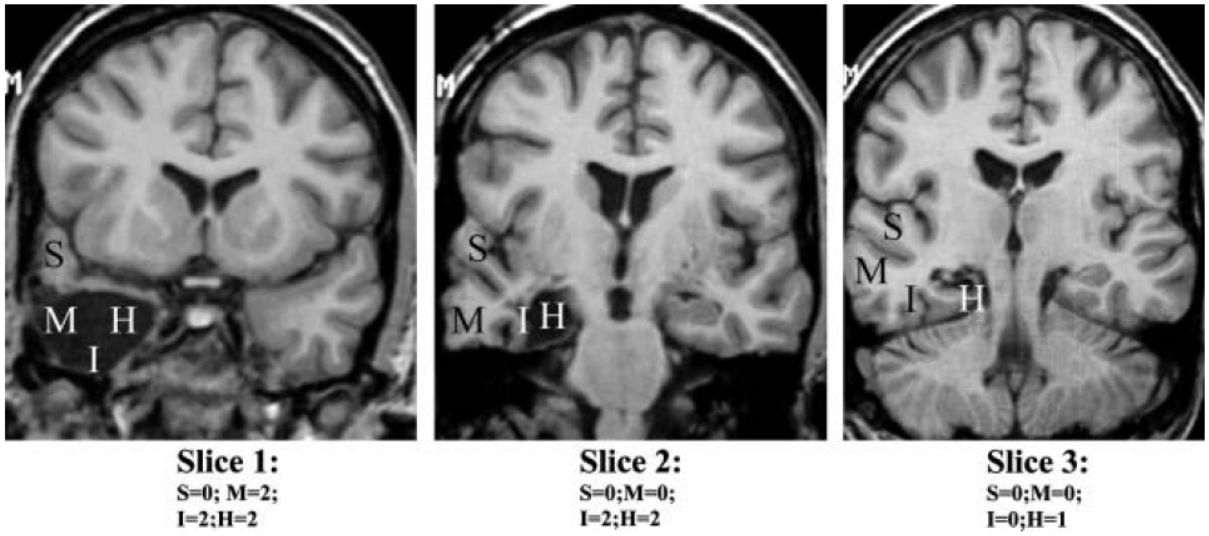

Fig 5. *Coronal MRI-slices through the temporal lobe, after TLR. The resection points for the respective compartments are shown. (Slice 1: center of the optic chiasm; Slice 2: the first slice containing the pontomesencephalic junction and Slice 3: the first slice containing the fourth ventricle. S=superior; M=median, I=inferior and H=hippocampal compartments, respectively. 0= no resection; 1= 0-50% resection; 2= more than 50 % resection. Reprinted with permission.*

The extent of resection in each compartment was estimated visually and given a value between 0 and 2; 0 points for no resection; 1 point for a resection of less than 50 % and 2 points for a resection of more than 50% of the compartment (Fig 5). This made possible an estimation of the resection made in 12 different parts of the temporal lobe, with a resection point for each individual compartment. The method was partly adapted from Katz et al [73]. The number of patients with and without resection in each compartment

and with and without VFD was compared. An average resection point for each compartment in the ATL and MATL groups with and without VFD was calculated by dividing the sum of the resection points in the respective compartments for each group by the number of subjects in each group. An interrater reliability study of the method was performed by independently assessing resection points in 252 compartments in 21 of the MRIs.

2.2 STUDY II

Seven healthy volunteers (four females) without any history of neurological or psychiatric disorder were recruited for this study. Age range was 23-62 years (mean 33.1). In addition, two patients, 56 and 60 years old, who had undergone TLR for medically refractory TLE, more than 10 years prior to this study, were recruited. The patients had perimetry performed as part of the routine preoperative work-up, which was normal in both patients, and postoperative perimetry was performed more than three months postoperatively.

Diffusion tensor imaging

MRI studies were performed on a Philips Gyroscan Intera 1.5 T release 9 with research software functionality HARDI (High Angular Resolution Diffusion Imaging, Philips, Eindhoven, the Netherlands). DTI of the whole brain was performed with isotropic 2.2 x 2.2 x 2.2 mm voxels, b=0 s/mm^2 plus 15 diffusion-sensitizing gradient directions (b=800 s/mm^2). Reconstructed pixel size was 1.9 x1.9 mm for both DTI images. Further details on the DTI acquisition can be found in paper II.

Data processing and tractography

Fractional anisotropy maps and tractography were generated by research software PRIDE with fibre tracking tool V4 (Philips, Eindhoven, Netherlands) on a standard PC according to the method described by Mori et al [120, 121]. Anisotropy maps were superimposed on the b=0 images. After identifying the lateral geniculate nucleus on the coronal T1-weighted images using anatomical references (lateral and caudal to the pulvinar of the thalamus) we changed to the color-coded fractional anisotropy map [122, 123]. By stepping one to two slices anteriorly we could identify a region with a high FA (>0.5), typically containing voxels dominated by green color (fibres running in an anterior-posterior direction). The first region of interest (ROI) was placed to include all these voxels to track fibres coming from the lateral geniculate nucleus coursing anteriorly but carefully outlined not to include fibres of the adjacent fibre tracts (Fig 6). A second ROI was placed at the level of the occipital horn of the lateral ventricle including the so-called “stratum sagittale”, which contains both geniculocalcarine fibres in its lower part, but also other fibre tracts such as the inferior longitudinal fasciculus and inferior occipitofrontal fasciculus [122, 124]. A two-ROI tractography was made by one neuroradiologist (LJ) and one neurosurgeon (DN) [93, 94, 121]. Tractography was terminated when fractional anisotropy was less than 0.25. The distances between the most anterior extent of Meyer’s loop and the temporal pole and the tip of the temporal horn were measured by examining the frontal and axial slices on the b=0 slices.

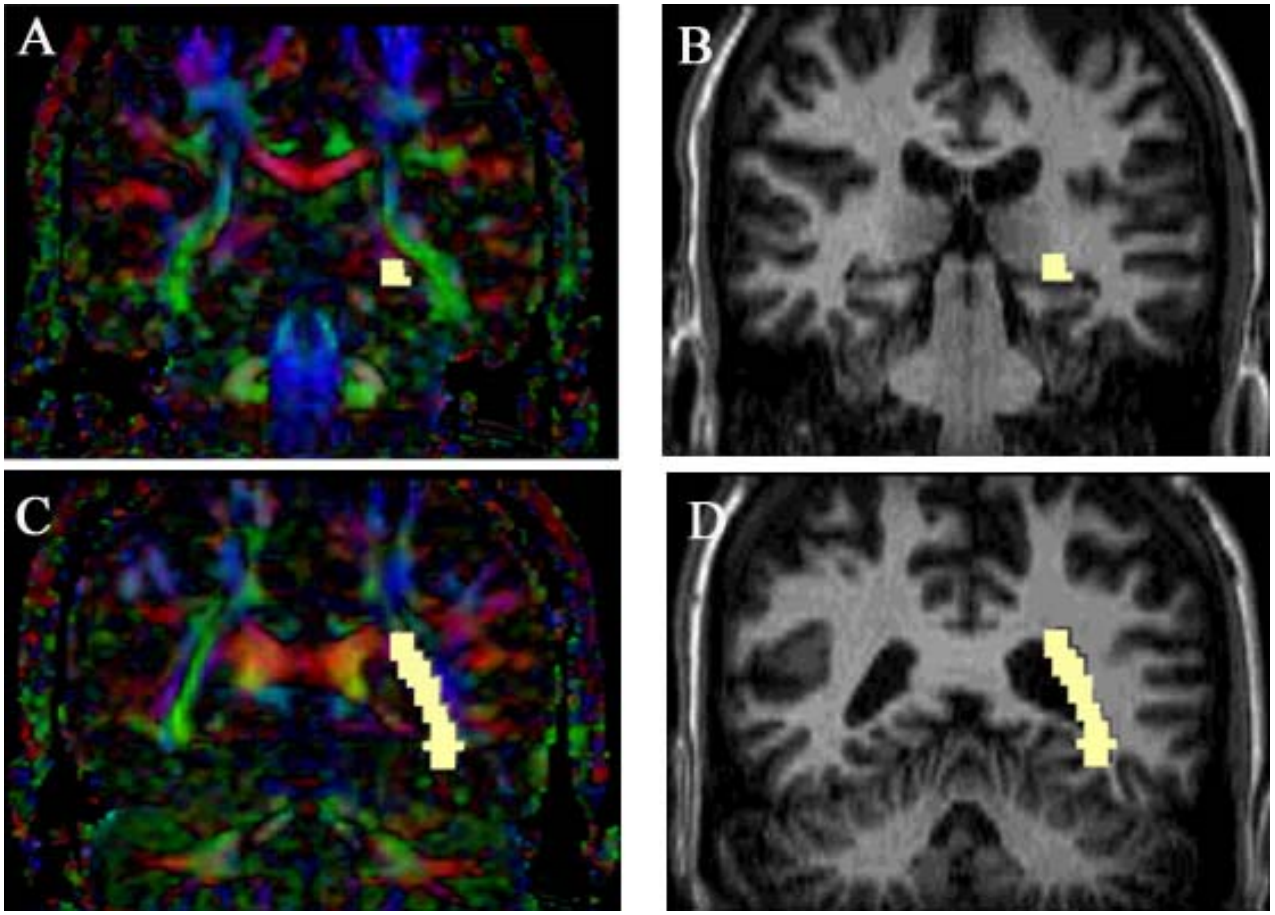

Fig 6. *Coronal slices anterior to the lateral geniculate nucleus (A, B) with regions of interest (in yellow) superimposed on a color-coded fractional anisotropy map (A) and on a T1-weighted image (B). Coronal slices at the level of the stratum sagittale (C, D) with regions of interest superimposed on a color-coded fractional anisotropy map (C) and a T1-weighted image (D). The color-code is red=left-right; blue=cranial-caudal, green=anterior-posterior.*

2.3 STUDY III

Eight children with TLE evaluated at The Hospital for Sick Children, Toronto, Canada, were included in the study. Six patients had medically refractory seizures and were evaluated for epilepsy surgery, the remaining two patients had infrequent seizures or were seizure-free on antiepileptic drug therapy. Their mean age was 12.8 years (range 5.9 – 17.3), there were three girls and five boys. Only patients with semiological and ictal and/or interictal EEG findings consistent with a lateralized temporal seizure focus were included. All children had an MRI of the brain including DTI. None had clinical seizures 24 hours prior to the MR examination. Clinical and radiological findings are shown in Table 1. Ten healthy age-matched children without any neurological symptoms and with

no history of seizures formed the normal control group. These children were recruited as controls for a separate study. Their mean age was 12.9 years (range 9.5-17.2), there were seven girls and three boys.

Table 1. *Clinical and radiological findings in eight children with temporal lobe epilepsy investigated by DTI.*

No	Gender	Age (yrs)	Duration of epilepsy (yrs)	Clinical data (seizure type, frequency, developmental history)	Location of Sz focus based on EEG	MRI findings (Histopathology when available=*)
1	female	5.9	0.6	CPS:crying/upset-unresponsive, blanking out+ gibberish speech.	L temporal	L posterior parahippocampal low-grade glioma
2	male	17.4	2.4	Aura: sensation of arm squeezing + GTCS.	L temporal	Normal
3	male	6.3	4.3	CPS: "freezing" + eye and head deviation to left + vocalization; Stiffening and jerking bilateral.	R temporal	Normal (microdysgenesis, gliosis in medial temporal lobe *)
4	male	16.1	15.1	CPS: staring spells + anxiety attacks + fall + tonic posturing.	L temporal	L hippocampal sclerosis (Subpial gliosis *)
5	male	8.2	2.2	CPS: ringing in ears then right arm stiffening	L temporal	L temporal cortical lesion FCD/DNET
6	female	15.9	9.9	CPS: Staring+hand automatism. Nocturnal sz with oral and/or hand automatisms	L frontotemporal	Normal
7	male	15.5	5.5	CPS: Freezing, staring,unresponsive, drooling,	L temporal	L FCD
8	female	17.3	1.3	CPS: Burning smell + tingling in right hand, GTCS, nauseating feeling in stomach, drooling	L temporal	L hippocampal sclerosis (MTS + gliosis in temporal pole*)

Sz=seizure; CPS=complex partial seizures; GTCS=generalized tonic-clonic seizures; L=left; R=right; DNET=dysembryoblastic neuroepithelial tumor; Nps =formal Neuropsychological assessment FCD= focal cortical dysplasia; MTS=mesial temporal sclerosis)

DTI acquisition
DTI was performed on a 1.5 T GE Signa LX (General Electric, Milwaukee, WI , USA) scanner using quadrature head coil, single shot diffusion-weighted echo planar imaging. Twenty-five axial contiguous slices were obtained aligned to the anterior commissure - posterior commissure line to cover the whole brain, giving a total imaging time of 4 min 40 s. At each slice position, in addition to b=0 images, a single b-value of 1000 s/mm^2 was applied in 25 spatially isotropically arranged non-collinear directions, with the following parameters: TR=10000 msec, TE=113 msec, FOV= 26 cm and matrix of 128 x 128. Slice thickness was 4 or 5 mm.

Data processing and tractography
Post processing of diffusion tensor metrics including FA, trace, and the three eigenvalues were calculated and tractography carried out using DTIStudio V 2.4 (Johns Hopkins Medical Institute, Laboratory of Brain Anatomical MRI, http://lbam.med.jhmi.edu/) [93, 125]. The major eigenvalue, equivalent to the diffusivity parallel to the principal axis of the fibres was expressed as the parallel diffusivity, $\lambda_{\parallel}$. The diffusivity perpendicular to the principal diffusion direction was expressed as the perpendicular diffusivity, $\lambda_{\perp} = (\lambda medium + \lambda minor)/2$.

Quantitative analysis
For the assessment of temporal lobe white matter (TLWM), a region of interest (ROI) was drawn on the axial slice where the optic tract and mamillary bodies could be identified on the b=0 image (Fig 7). The ROI placement was guided by b=0 and color-coded FA maps so as to include the central temporal lobe white matter. This ROI was used as a seed ROI for fibre tracking using the FACT algorithm to produce a volume of interest (VOI) containing a larger number of voxels, in a similar way as described by Concha et al [108]. The FA threshold used for the fibre tracking was 0.2 and the maximum turning angle was set to 45 degrees. Tracked voxels that were outside the lobe of interest such as in the frontal lobe were deleted manually. For the assessment of cingulate gyrus white matter (CGWM), another ROI was placed on an axial slice cranial to the corpus callosum on the color-coded FA maps, where the white matter of the cingulate gyrus can be seen running in an anterior to posterior orientation. This ROI was used as a seed ROI for fibre tracking to produce a VOI in the CGWM. The mean FA, trace, $\lambda_{\parallel}$ and $\lambda_{\perp}$ were measured for the VOI of the TLWM and CGWM.

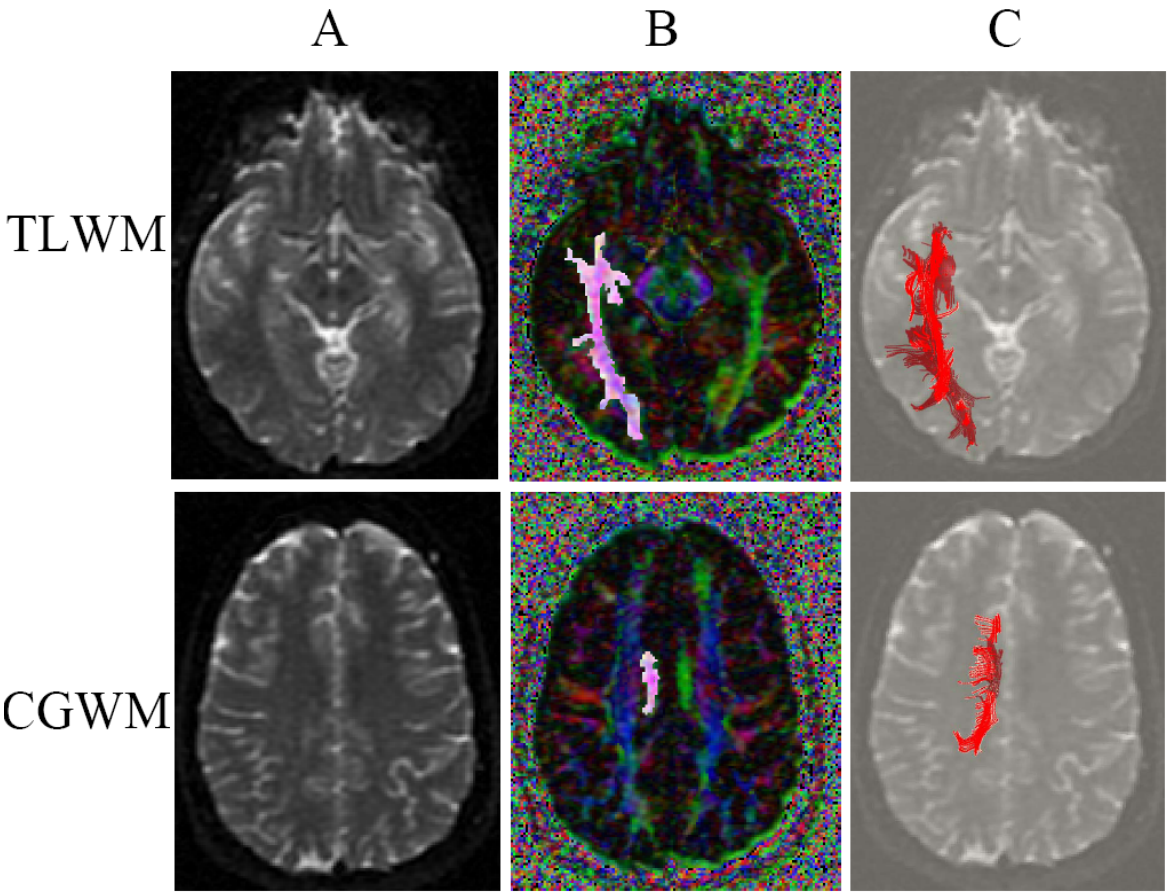

Fig 7. *(Case 8). A: Axial b=0 images; B: Axial color-coded FA map with the seed ROI outlined and C: Axial b=0 images with the resulting tractography for the temporal lobe white matter (TLWM, first row) and cingulate gyrus white matter (CGWM, second row). A hyperintense lesion is seen in the left medial temporal lobe on the b=0 images, in keeping with hippocampal sclerosis. The diagnosis was confirmed by histopathology.*

2.4 STUDY IV

Eleven children referred for follow-up MR imaging for a supratentorial lesion with features of low-grade tumor at The Hospital for Sick Children, Department of Diagnostic Imaging, Toronto, Canada, were recruited into the study. Nine had epilepsy, the remaining two had either no seizures, or presented with a single epileptic seizure. Mean age was 11 years (range 3 – 17 years). There were five males and six females. Further details of the clinical findings are shown in Table 2. All tumors demonstrated well-demarcated margins with no evidence of edema or necrosis on MR imaging. Calcification was present in six cases. The radiological diagnoses included ganglioglioma, DNET, pilocytic astrocytoma and low-grade astrocytoma (WHO grade II). Tissue diagnosis was available in four cases and were DNET (case 8), astrocytoma grade II (case 10), pilocytic astrocytoma (case 11) and epidermoid tumor (case 5). Mean duration of follow-up on imaging was 1.8 years (range 0.2– 7.8 years).

DTI acquisition

MR and DTI were performed on the same scanner, using the same imaging parameters as described for study III. Structural MR for the patient group included T1, T2, dual echo, FLAIR and 3D T1 SPGR sequences.

Data processing and tractography

Post processing of diffusion tensor metrics, the generation of color vector orientation maps and tractography using the FACT algorithm were carried out on DTIStudio V 2.4 (Johns Hopkins Medical Institute, Laboratory of Brain Anatomical MRI, http://lbam.med.jhmi.edu/). The fractional anisotropy (FA), the diffusivity, expressed as trace, and the major, medium and minor eigenvalues were calculated. The tracking was terminated when the trajectory reached a voxel with FA less than 0.2 or when the angle between two consecutive steps was greater than 50^{o}.

Table 2. *Clinical presentation and gradings of white matter tracts in children with low grade supratentorial tumor.*

Case/Age/ Gender	Tumor location	Clinical data	Follow-up duration	Projection tracts	Association tracts	Commissural tracts
1/3/F	R frontal	Focal epilepsy since age 3. No neurological deficit.	10 months	CST: 1b	1a	1a
2/17/M	L temporal	Headache, no seizures. No neurological deficit	3 months	1a	SS: 2b	1a
3/10/M	R Postcentral gyrus	Focal epilepsy since age 9. No neurological deficit	2 months	CST 1 b	SLF: 1b	1a
4/6/F	L mesial temporal	Epilepsy since age 6. No neurological deficit	3 months	1a	SS: 1b	1a
5/17/F	L frontotemporo-parietal junction	One seizure at age 7. No neurological deficit.	9 years	CST 2b	SS:2b	Fmajor:1b
6/14/F	L frontal operculum	Focal epilepsy since age 13. No neurological deficit	9 months	1a	1a	1a
7/15/F	R temporal lobe	Epilepsy since age 14. No neurological deficit	10 months	1a	SS: 1b	1a
8/11/M	R frontal	Epilepsy since age 6. No neurological deficit	4,5 years	ATR: 2b	IFO: 2b	Fminor: 2b
9/7/M	L parietal	Epilepsy since age 18 months. No neurological deficit	6 years	CST/CPT: 2b	SLF: 2b	1a
10/12/F	R temporal	Epilepsy since age 12. No neurological deficit	2 months	1a	ILF: 1b	1a
11/16/M	R occipital	Epilepsy since age 15, No neurological deficit	5 months	1a	SS: 1b	Fmajor: 1b

CST=corticospinal tract; CPT=corticopontine tract; ATR=anterior thalamic radiation; SS=sagittal stratum; SLF=superior longitudinal fasciculus; ILF=inferior longitudinal fasciculus; IFO=inferior fronto-occipital fasciculus; Fmajor=forceps major; Fminor=forceps minor.

Quantitative analysis

The anatomical images were reviewed to identify the location of the lesion prior to placing regions of interest (ROI). ROIs were placed by one pediatric neuroradiologist (EW) and one neurosurgeon (DN). The axial slice with the largest anterior-posterior and right-left tumor diameter was selected for ROI placement. Three identical elliptical ROIs, measuring 21 pixels each, were placed in every case. One ROI was placed in the tumor, avoiding areas that demonstrated calcification, which showed as low signal on the b=0 images. A second identical ROI was placed in the white matter adjacent to the tumor and on the same axial slice as the ROI placed in the tumor. A third ROI was placed in the white matter on the contralateral normal appearing side, on the same slice and at the same anatomical location as the ROI placed in the white matter adjacent to tumor. The ROIs were placed on the b=0 images and then transposed onto anatomically coregistered positions on the FA, trace and eigenvalue maps (Fig 8). The mean values of FA, trace, λmajor, λmedium, λminor values were measured.

Semi-quantitative analysis

The association, projection and commissural tracts were assessed from the directional color vector maps, guided by published data [99]. The major projection tracts included the anterior thalamic radiations and corticospinal/corticopontine tracts. The commissural tracts included the forceps major and forceps minor of the corpus callosum. The association tracts included the superior longitudinal fasciculus, inferior longitudinal fasciculus, inferior frontooccipital fasciculus and superior frontooccipital fasciculus. There was considerable overlapping of the inferior longitudinal fasciculus, optic radiation and inferior occipitofrontal fasciculus in the region of the trigone, therefore these tracts were classified as the sagittal stratum.

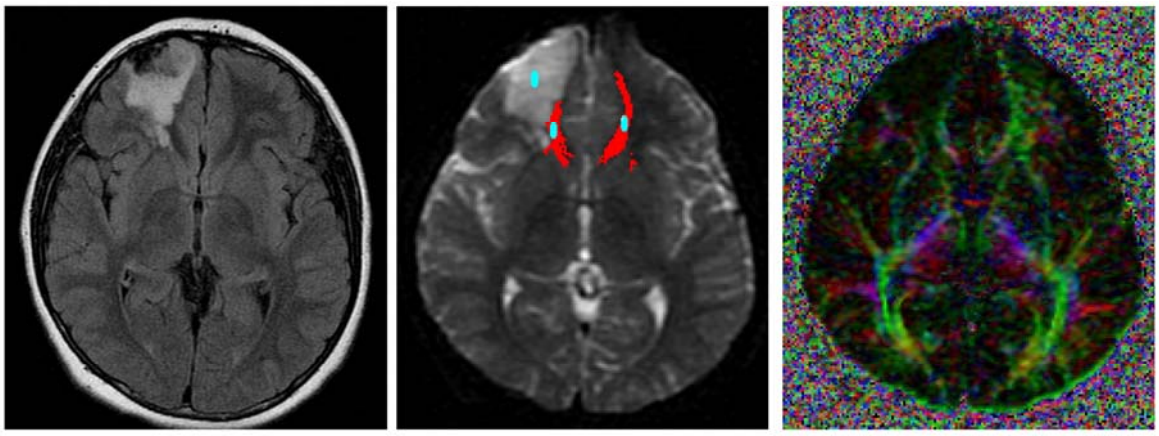

a b c

Fig 8. *Case 9. (a) Axial FLAIR image showing a well-defined tumor in the right frontal lobe that extends across the cerebral mantle to the ventricular margin. Biopsy performed at an outside institution demonstrated dysembryoplastic neuroepithelial tumor (DNET). (b) Axial b=0 image showing the three regions of interest (ROI) used for the quantitative analysis. The ROIs were placed within the tumor, in the white matter adjacent to the tumor and the contralateral normal appearing side. (c) Color-coded FA map and (b) tractography demonstrate grade 2 b pattern, that is, displacement and reduction in size of the forceps minor of the corpus callosum. Reprinted with permission.*

The white matter tracts were graded based on the size, color hue and displacement of the tracts on all axial color vector maps [126]. The tracts were visually inspected and graded by two raters by consensus. Grade 1 was characterized by normal tract size and normal color hue on the color vector map compared to the contralateral side and normal appearance of the tract on tractography. Grade 2 was characterized by reduced tract size but preserved color hue on the color vector map compared to contralateral side and reduced tract size on tractography. Both grade 1 and 2 were further subdivided to “a” or “b” depending on the absence or presence of displacement of the white matter tracts

respectively. Grade 3 was characterized by loss of the directional color hue on color vector map along all or part of the tract and failure of tracking on tractography.

2.5 STATISTICAL METHODS

In study I the interobserver agreement was calculated as described by van den Berge and a κ value of more than 0.6 was considered acceptable[127]. The X_2-test was used for statistical analysis of the data in Table 4. In study III a paired t-test was used to compare data between the left and right side in the control group and between the seizure focus side and the contralateral side in the patient group. This analysis was repeated for mean FA, trace, $\lambda_{\parallel}$ and $\lambda_{\perp}$ of the TLWM and CGWM. After the initial analysis showed no differences between sides the data was aggregated into one TLE group and one control group, regardless of sides, and further analysis was done using this data. The mean FA, trace, $\lambda_{\parallel}$ and $\lambda_{\perp}$ of the TLWM and CGWM of the TLE patients were compared to the data from normal controls using the Generalized Estimation Equation to account for repeated measurements within each subject. Bonferroni correction was done to reduce type I error and a p value of <0.01 was considered statistically significant. In study IV the inter-rater agreement on FA, trace, λmajor, λmedium and λminor of the tumor, the white matter adjacent to the tumor and the normal contralateral side were evaluated using intraclass correlation coefficient. Intraclass correlation coefficient of 0–0.2 indicated poor agreement, 0.21–0.40 fair agreement, 0.41–0.60 moderate agreement, 0.61–0.8 substantial agreement, and 0.81–1.0 nearly perfect agreement. The average of the measurements acquired was used for further analysis. The FA, trace, λmajor, λmedium and λminor of the tumor and of the white matte adjacent to the tumor were compared to the normal contralateral side using a paired t-test. P-values less than 0.05 were considered statistically significant.

3. RESULTS

The principal findings of each study are listed below, followed by a detailed description of the results for each study:

Study I: A VFD was found in 50% of the patients after TLR and the VFD frequency was similar for both ATL and MATL.

Study II: A considerable variability in the anterior extent of Meyer´s loop, similar to what has been reported in dissection studies was found. Meyer´s loop was found to be more posteriorly located than in dissection studies. Tractography could demonstrate an injury to Meyer´s loop in one patient with quadrantaniopa.

Study III Children with TLE have bilaterally increased diffusivity but preserved anisotropy in the temporal lobe and cingulate gyrus white matter compared to controls.

Study IV: White matter tracts adjacent to supratentorial low-grade tumors in children have preserved structural integrity.

3.1 STUDY I

Frequency of VFD
Twenty-five of the patients (50%) developed a VFD, 16 (48%) in the ATL group and nine (53%) in the MATL group. The VFDs occurred in the homonymous, upper, contralateral quadrant in 24 patients and one patient developed a contralateral hemianopia. The frequency of seizure-free patients was similar for both procedures with 60% seizure free in the MATL group compared to 63% in the ATL group. However, only 13% of the patients in the MATL group had a seizure reduction of < 75%, compared to 37% of the patients in the ATL group.

MRI analysis
Thirteen patients had surgery on the left side and 21 patients on the right side. Nineteen patients had an ATL and 15 patients had a MATL. There was a difference in average resection points for the studied compartments between ATL and MATL reflecting the larger lateral resection in ATL and the more extensive hippocampal resection in MATL (Table 3). No significant correlations between occurrence of resection in a compartment (resection point >0) and the presence of a postoperative VFD were found in any compartments, except in the superior compartment in the M1 slice (M1Sup) ($p<0.02$) (Table 4).

Table 3. *Average resection score for all compartments. The results are shown for MATL and ATL with and without VFD.*

Surgical approach	VFD	Average Resection Point											
		S1sup	**S1med**	**S1inf**	**S1hip**	**S2sup**	**S2med**	**S2inf**	**S2hip**	**S3sup**	**S3med**	**S3inf**	**S3hip**
MATL	**No (n=8)**	0,13	1,6	1,9	1,9	0	0	0,5	2	0	0	0	0,63
	Yes (n=7)	1	2	2	2	0	0,43	0,71	1,57	0	0	0,14	0,57
ATL	**No (n=11)**	1,36	2	2	1,9	0,27	0,63	0,81	0,91	0,09	0,27	0,18	0
	Yes (n=8)	1,38	2	2	1,9	0,38	0,88	1,1	0,88	0,13	0,25	0,25	0,25

(VFD=visual field defect; ATL= anterior temporal lobe resection; MATL= modified anterior temporal lobe resection; (S1: Slice 1 (center of the optic chiasm); S2: Slice 2 (the first slice containing the pontomesencephalic junction) and S3: Slice 3 (the first slice containing the fourth ventricle). sup=superior; med=median, inf=inferior and hip=hippocampal compartments, respectively)

Table 4: *Frequency of VFD in patients with and without resection in the S1Sup compartment.*

Resection in S1 Sup	VFD	No VFD
Yes	14	11
No	1	8

(VFD=visual field defect; S1Sup= superior compartment in the coronal slice through the optic chiasm)

3.2 STUDY II

Intersubject variability in the anatomy of Meyer´s loop

Mean distance from the temporal pole to the anterior edge of Meyer's loop was 44 mm on both sides and the range was 34-51 mm on the right side and 35-49 mm on the left side. The mean distance from the temporal pole to the tip of the temporal horn was 28 mm (range 27-30 mm) on the right side and 29 mm (range 25-30 mm) on the left side. Meyer's loop did not reach the tip of the temporal horn in any subject and the anterior edge of Meyer´s loop was on average 16 mm (range 8-21 mm) posterior to the tip of the temporal horn of the lateral ventricle.

Tractography after temporal lobe resection

In Patient A, who had developed a postoperative contralateral upper quadrantanopia, tractography revealed a reduction of the anterior extent of Meyer's loop on the side of the resection. On the non-resected side Meyer's loop was found to be 40 mm behind the temporal pole and 10 mm behind the tip of the temporal horn. The extent of the lateral resection was 53 mm measured from the anterior margin of the temporal fossa.
In Patient B where no postoperative visual field defect could be demonstrated, tractography did not show any signs of damage or disruption of Meyer's loop. Meyer's loop was found to be 51 mm posterior to the anterior margin of the temporal fossa on the side of resection, 49 mm behind the temporal pole, and 15 mm posterior to the tip of the temporal horn on the non-resected side. The extent of the lateral resection in patient B

was 42 mm. The results from the tractography and the corresponding perimetry results for patients A and B are shown in Fig 9.

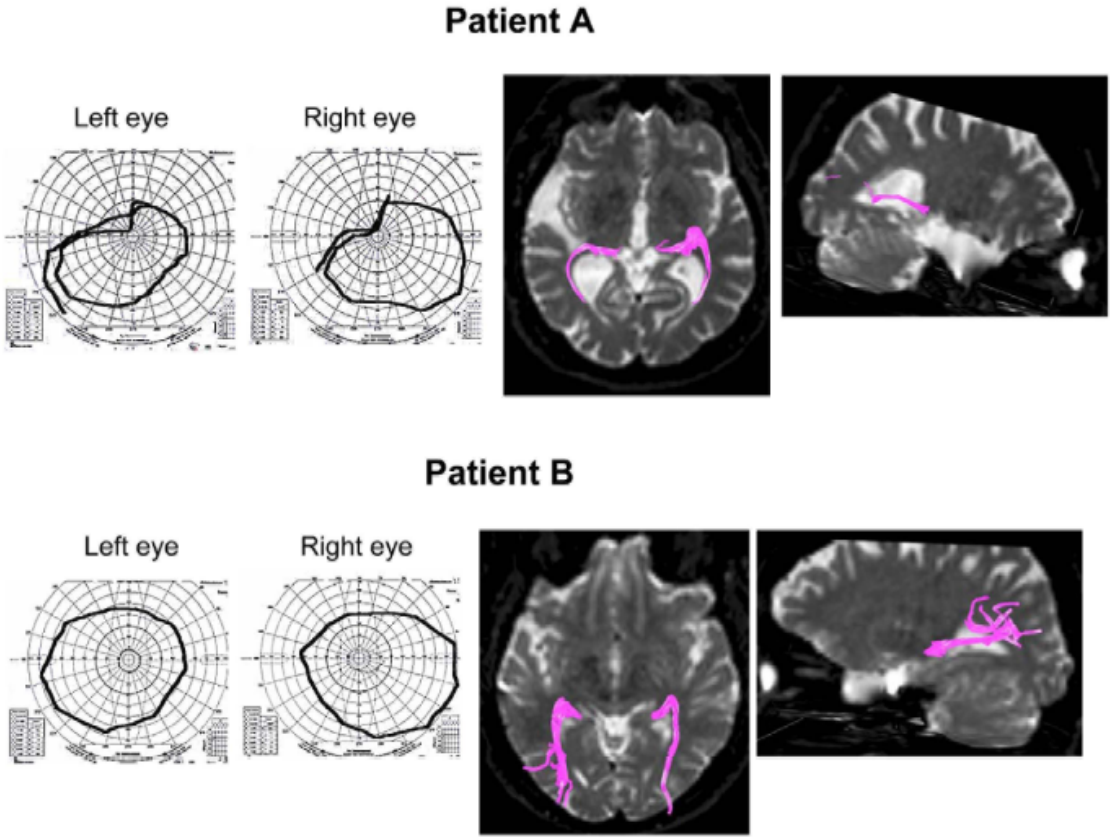

Fig 9. *Patient A: Postoperative perimetry demonstrating a left homonymous superior quadrantanopia. The axial view with the postoperative tractography demonstrates a disruption in Meyer's loop on the right side. The sagittal view shows the relationship between the resection and tractography of Meyer´s loop.*
Patient B: No postoperative visual field defect, and Meyer´s loop is intact on the axial view. The sagittal view shows that the resection does not reach Meyer's loop. Reprinted with permission.

3.3 STUDY III

Patient characteristics
Mean age at seizure onset was 7.9 years and the mean duration of epilepsy was 5.2 years. Five children had complex partial seizures only (cases 1, 4, 5, 6 and 7) and two children had complex partial seizures with infrequent secondary generalization (cases 3 and 8). One child had frequent auras and infrequent generalized seizures (case 2) (Table 1). The seizure focus was on the left in seven patients and on the right in one patient. Three children had TLR and the histopathology showed microdysgenesis and gliosis in the medial temporal lobe (case 3, normal MRI), subpial gliosis (case 4, hippocampal

sclerosis on MRI) and mesial temporal sclerosis and gliosis in temporal pole (case 8, hippocampal sclerosis on MRI).

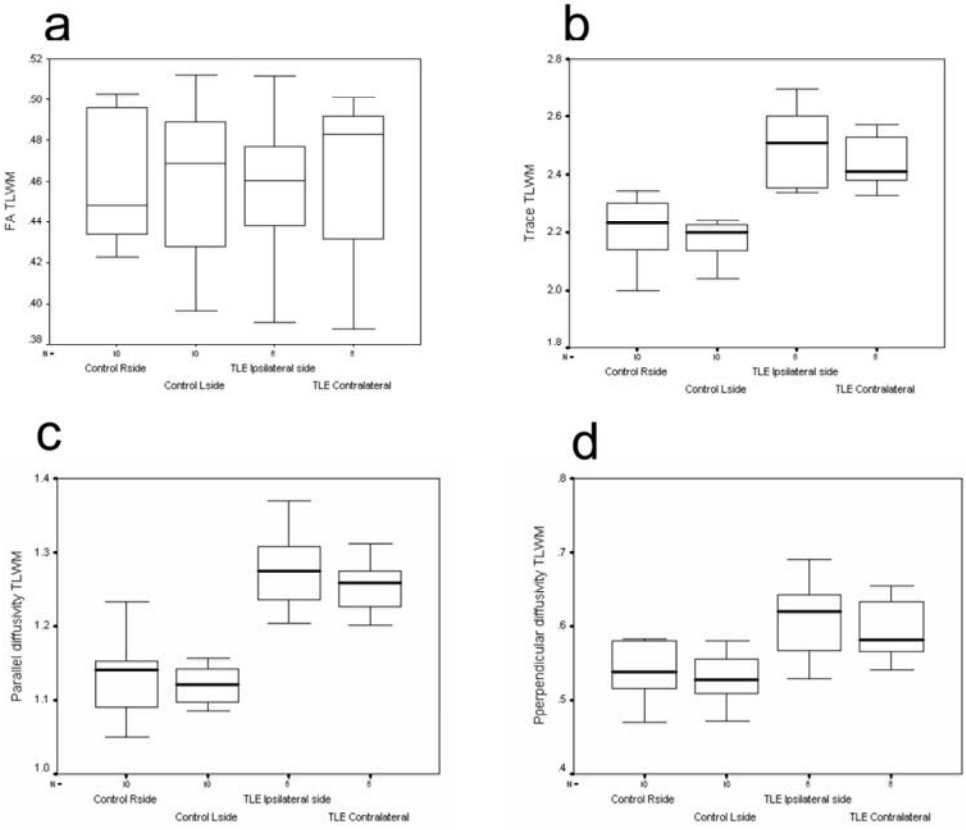

Fig 10. *Boxplots of (a) FA, (b) trace, (c) parallel diffusivity and (d) perpendicular diffusivity of the temporal lobe white matter (TLWM) of controls and temporal lobe epilepsy patients.*

Quantitative analysis

There were no significant differences in FA, trace, $\lambda_{\parallel}$ and $\lambda_{\perp}$ between the left and right sides in the control group. Similarly, no significant differences in FA, trace, $\lambda_{\parallel}$ and $\lambda_{\perp}$ were seen between seizure focus side and the contralateral side of the TLWM or CGWM in the patient group ($p>0.05$) (figs 10 and 11). TLE patients had significantly increased trace, $\lambda_{\parallel}$ and $\lambda_{\perp}$ values ($p<0.01$), but no significant difference in FA ($p>0.05$) in the TLWM compared to normal controls. Correspondingly, there were increased trace, $\lambda_{\parallel}$ and $\lambda_{\perp}$ values ($p<0.01$) but no significant difference in the FA ($p>0.05$) found in the CGWM in the TLE patients compared with controls.

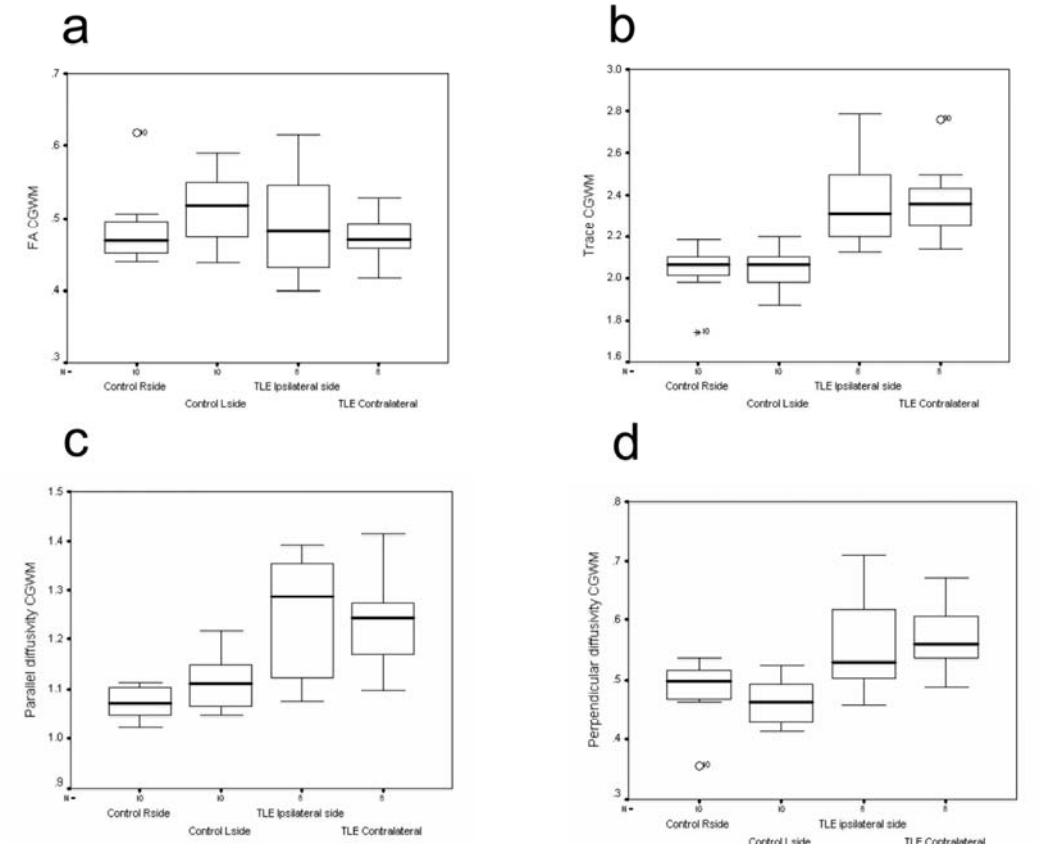

Fig 11. *Boxplots of (a) FA, (b) trace, (c) parallel diffusivity and (d) perpendicular diffusivity of the cingulate gyrus white matter (CGWM) of controls and temporal lobe epilepsy patients.*

3.4 STUDY IV

Tumor characteristics

The location of the tumors were as follows: three in the frontal lobe, four in the temporal lobe, two in the parietal lobe, one in the occipital lobe and one with a temporo-parietal localisation. The maximal dimension of the tumor in the axial plane varied from 13 to 48 mm (mean 29 mm).

Quantitative analysis of white matter adjacent to tumor

The intraclass correlation coefficients were higher than 0.6 in 12 of the 15 parameters measured. There was no significant difference between the FA, trace, and eigenvalues of the WM adjacent to the tumor and the normal contralateral WM ($p>0.05$). The FA of the tumor was significantly lower than the FA of the adjacent WM ($p<0.05$) and the normal contralateral side ($p<0.05$). The trace, λmedium and λminor values of the tumor were significantly higher than the trace, λmedium and λminor values of the adjacent WM ($p<0.05$) and of the normal contralateral side, ($p<0.05$) respectively.

Semi-quantitative analysis of white matter tracts

Four patients had grade 2b pattern of WM tract changes, that is, displacement of tract and reduced tract size. Six cases had grade 1b, that is, normal size but displaced WM tracts (Fig 12). One patient was classified as grade 1a with normal tract size and color hue in all analyzed tracts.

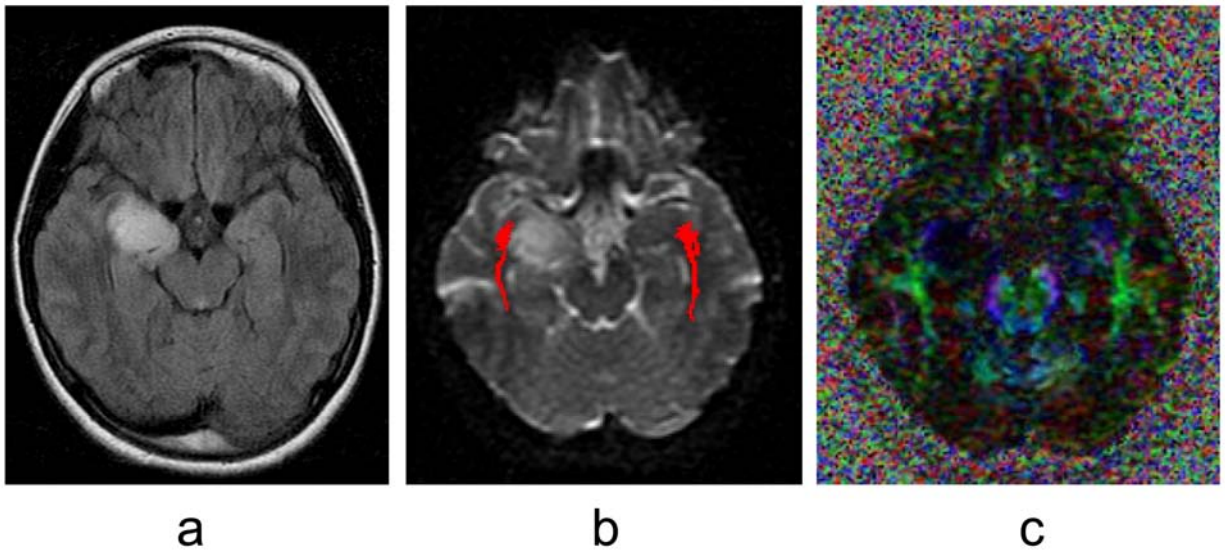

Fig 12. *Case 10. (a) Axial FLAIR images showing a tumor in the right mesial temporal lobe involving the anterior hippocampus, uncus and amygdala. Histopathology demonstrated astrocytoma grade II. (b) tractography overlaid on a b=0 image shows slight lateral displacement but symmetrical size of the inferior longitudinal fasciculus, consistent with grade 1b. (c) Color-coded FA map of the same axial slice. Reprinted with permission.*

4. DISCUSSION

4.1 FREQUENCY OF VISUAL FIELD DEFECTS AFTER SURGERY FOR TLE

In our TLR series of 50 patients, 25 developed a postoperative VFD. Previous studies of the frequency of VFD after classical anterior TLR report a VFD in 52 to 100 percent of patients, usually well above 60 percent [72, 75-77, 128]. The differences in VFD frequency may be attributed to methodological issues when measuring the visual fields or differences in the surgical procedure used. The VFDs detected were located in the contralateral homonymous upper quadrant, or in a part of a quadrant, in 24 of 25 patients. One patient developed hemianopia, probably due to injury to the optic tract.

4.1.1 Lateral resection size does not predict VFD frequency

We found no difference in VFD frequency after ATL and MATL and thus no correlation between lateral extent of resection and VFD frequency. Several other studies using either intraoperative measures [75, 128, 129] or postoperative imaging [73] to assess the extent of resection have reported similar results, with no correlation between frequency of VFD or size of the VFD and the lateral resection size. However, other studies have reported approximate correlations of field loss with intraoperative resection length [77] and with postoperative MRI and automated static perimetry [72, 130]. A recent study measuring lateral resection size on axial MR images and the area of the VFD found them to have a linear correlation, where every 10 mm of lateral resection would add 20 % loss of vision in the quadrant [78]. In this study, however, only patients with VFD were included, which may introduce a sample bias, and the regression analysis the investigators used assumes that an approximate linearity holds to the anterior limit of Meyer's loop, which may not be the case. The issue of a possible relationship between the extent of the lateral TLR and freuqency of VFD is thus not settled. The difficulty in finding such a correlation is probably due to a considerable interindividual variation in the anterior extent of Meyer´s loop [119]. In Study II, using tractography, we reported a 17 mm intersubject variability in the anterior extent of Meyer's loop. These results are similar to data from two previous dissection studies, and data from a histological study, all three reporting a 15 mm variability in the anterior extent of Meyer's loop [85, 119, 131]. The similarity of results from three different methodologies suggests that there is indeed an intersubject variability in the anterior extent of Meyer´s loop, and that it is of the order of 15 mm.

4.1.2 Approach to the temporal horn may influence VFD frequency

VFD is common not only after TLR, but also following amygdalohippocampectomy, occurring in 79 % in transcortical amygdalohippocampectomy as compared to 73 % after TLR in the same study [71]. SAHE has similar results with 83 percent of the patients developing a partial or complete quadrantanopia in a study of 54 patients [132]. This is at first look surprising, as SAHE per definition does not include the lateral temporal lobe. When considering the detailed anatomy of Meyer´s loop and the surgical techniques for TLR and SAHE there may however be an explanation for this. Meyer´s loop is a thin sheet of fibres, forming a slightly slanting roof of the temporal horn of the lateral ventricle (Fig 13). All procedures for removal of the mesial temporal lobe structures from a lateral approach, such as ATL, MATL and SAHE must enter the temporal horn of the lateral ventricle to gain access to the hippocampus. In other words, if the temporal horn is

opened through its roof, the incision will be very close to Meyer´s loop. From this follows that the extent of lateral resection is not necessarily as important as how the temporal horn is entered, and the anatomical relationship between the tip of the temporal horn and Meyer´s loop. In Study I we found a correlation between resection of the superior temporal gyrus and occurrence of a VFD. This may reflect that a resection of the superior temporal gyrus suggests a slighty more cranial resection, allowing for a more superior angle of incision through the roof of the temporal horn, resulting in injury to the optic radiation. This may also explain the high frequency of VFD seen in SAHE, as the angle of approach to the temporal horn, through the sylvian fissure, is even more from above than the approach through the superior temporal sulcus (Fig 13).

4.2 ANATOMICAL VARIABILITY AND ANTERIOR EXTENT OF MEYER´S LOOP

The distance from the temporal pole to the anterior rim of Meyer´s loop has been extensively discussed. The current study using DTI and tractography found Meyer´s loop to be located a mean of 44 mm (range 34-51 mm) behind the temporal pole. Meyer´s loop did not reach the tip of the temporal horn in any of our subjects. Findings similar to ours have been reported in a previous tractography study by Yamamoto et al, reporting the anterior extent of Meyer's loop to be a mean of 37 mm behind the temporal pole in five healthy volunteers [82]. This is more posterior than what has been described in both dissection studies (mean 27 mm) [119], histological staining studies (mean 23 mm) [85] and some of the lesional studies (24 mm) [78].

Kier et al, combining dissection and MRI, concluded that Meyer´s loop did not reach the tip of the temporal horn, thus supporting tractography studies [86, 87]. In contrast, Sincoff et al in a dissection study found that the optic radiation covered the entire lateral aspect of the temporal horn including the anterior tip along its lateral half [133]. They defined two anatomical surgical paths to the temporal horn that would avoid the optic radiations, the first a transsylvian anterior medial approach and the second a pure inferior path through the fusiform gyrus. They concluded that lateral approaches to the temporal horn through the superior and middle gyri, would traverse the optic radiations. However, their conclusions contradict data from lesion studies where transsylvian approaches have a high VFD frequency [132], and lateral approaches do not always cause a VFD (Study I).

The reasons for these diverging results are probably attributable to the different methods used to visualize the optic radiation. Tractography may have difficulties tracking fibres thinner than the voxel size at the edge of Meyer's loop, and may thus underestimate the anterior extent of Meyer's loop. On the other hand, dissection studies may overestimate the anterior extent of the optic radiation, as these fibres may be impossible to separate from adjacent fibre tracts, such as the inferior longitudinal fasciculus and the uncinate fasciculus. Histological staining studies can trace the individual axons from their origin and along their course, however shrinkage of the specimen may influence measurements of anatomical distances. Clinical observations of the occurrence of visual field defects following TLR rarely report visual field defects occurring in resections extending less than 30 mm from the temporal pole, which suggests that the anterior extent of Meyer's loop in most subjects is behind this point. This is exemplified by Patient B in study II

where no postoperative visual field defect could be demonstrated with a lateral resection of 42 mm and where Meyer's loop was found to be 51 mm posterior to the anterior margin of the temporal fossa on the side of resection.

4.3 IMPLICATIONS FOR TEMPORAL LOBE RESECTIONS

What implications for TLR could the data from this and other studies have to reduce the risk of a postoperative VFD? Both the anatomical configuration of Meyer´s loop as an outward slanting roof of the lateral ventricle and the variation in its position between patients have to be considered. Firstly, by selecting a more inferior approach to the temporal horn of the lateral ventricle, the risk of injury to the optic radiation might be decreased. The most extreme application of this is the subtemporal approach through the inferior temporal sulcus to the hippocampus, where no VFD:s were reported in seven patients [134]. A study comparing transsylvian, transtemporal and subtemporal approaches to tumors in the mesial temporal lobe found no VFD with the subtemporal approach, but new or worsened deficits in 20-45% of patients with the other approaches [135]. However, the subtemporal approach has other disadvantages such as the risk for temporal contusions, small field of view, and need for resection of the zygoma. Nevertheless, even using a regular TLR or SAHE, the angle of approach to the temporal horn of the lateral ventricle could be modified to be more anterior-inferior, avoiding the superior-lateral approach through the optic radiation (Fig 13,14).

4.3.1 Tractography of Meyer´s loop may reduce VFD frequency

The second consideration is to investigate the anterior extent of Meyer´s loop and its relationship to the temporal horn using DTI and tractography. This information may be used primarily in the preoperative risk assessment and possibly during surgery using neuronavigation. The intraoperative use of tractography may guide the surgeon both to avoid the optic radiation and to assess the orientation of the axons in the temporal lobe so that an incision in the white matter can be made parallel to rather than perpendicular to the axons, to minimize injury. Tractography should however be used more as a guidance to the approximate position to the optic radiation than an exact anatomical landmark, due to the current limitations in the technique. Before the role of tractography to map out the optic radiation in patients with TLE can be finally established, prospective studies with perimetry and DTI before and after TLR are needed. Therefore, such a study is currently ongoing at our institution. The aim is to determine the correlation between a postoperative visual field defect and the injury seen on tractography and clarify the intersubject variability in the anatomy of the optic radiation in patients with TLE. One should also bear in mind that the primary goal of TLR, i.e. to abolish the seizures, must not be compromised to save the optic radiation.

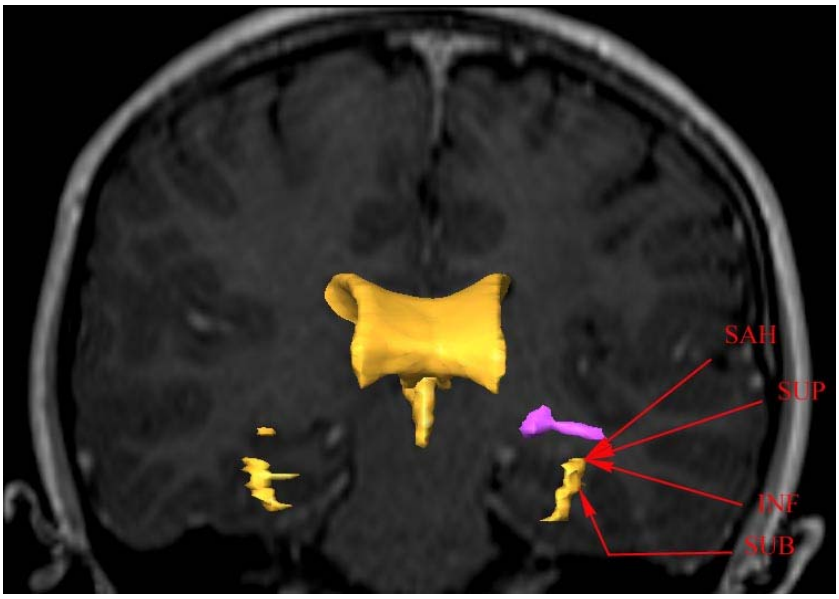

Fig 13. *Coronal, T1-weighted MRI showing the relationship between Meyer´s loop (in pink) and the temporal horn of the lateral ventricle. The anterior and temporal horns of the lateral ventricles and the third ventricle are outlined in yellow. The angle of approach to the temporal horn for a selective amygdalohippocampectomy (SAHE), TLR through the superior temporal gyrus (SUP), TLR through an inferior approach (INF) and the subtemporal approach (SUB) is shown.*

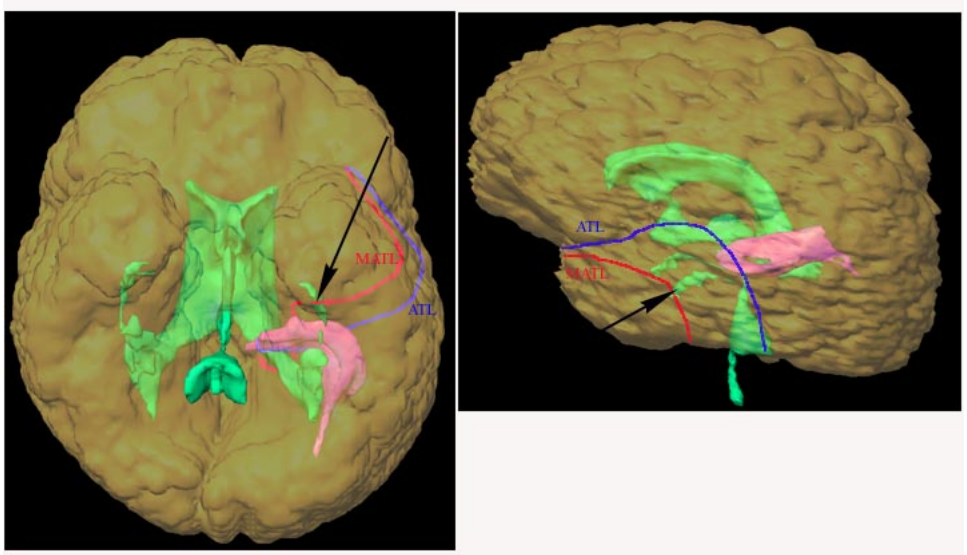

Fig 14. *Caudal and lateral views of the brain with the ventricular system reconstructed (in green) and Meyer´s loop on the left side in pink. The resection lines for a classical anterior temporal lobe resection (ATL) with a larger lateral extent and a modified ATL (MATL) which reaches more posteriorly in the mesial temporal lobe are shown. An anterioinferior approach to the temporal horn is indicated (arrow). The distance from the temporal pole to the temporal horn was 29 mm and from the temporal pole to the anterior rim of Meyer´s loop 46 mm in this subject. Meyer´s loop does not reach the tip of the temporal horn.*

4.4 DIFFUSION ABNORMALITIES IN CHILDREN WITH TLE

Children with TLE were found to have bilaterally elevated diffusivity with normal FA in both TLWM and CGWM. One previous DTI study of children with TLE found decreased FA in the hippocampus ipsilateral and contralateral to the seizure focus and increased diffusivity in the ipsilateral, but normal diffusivity in the contralateral hippocampus [37]. Increased diffusivity in the white matter in children with TLE has not been previously reported, but is consistent with studies in adult TLE patients where increased diffusivity in several white matter structures including the fornix, cingulum [108], external capsule, corpus callosum [109], and ipsilateral TLWM [35] has been found. The same studies, however, have reported a decreased FA in contrast to the preserved FA found by our study [35, 108, 109]. There may be several explanations for this discrepancy.

First, there are differences in histopathological findings in TLE between adults and children. Reduced FA in the white matter adjacent to cortical malformations in children with epilepsy has been reported [126]. In our study, only three children had a histopathological diagnosis, including microdysgenesis and gliosis in the medial temporal lobe, subpial gliosis and MTS and gliosis in temporal pole. In the remaining five patients two had normal structural MRI and three had subtle lesions suggestive of a focal cortical dysplasia, DNET or a low-grade glioma. As none of our patients had a widespread cortical malformation, this may explain the preserved FA. On the other hand, all adult TLE patients in previous studies had MTS [35, 108], suggesting that the reduction in FA is related to the epilepsy and not to the lesion. Nevertheless, the heterogeneity in the pathological substrates of our pediatric cohort with TLE may have been a confounder and resulted in relatively normal FA.

A second explanation for the difference in FA between adults and children may be the duration of TLE. Adults with medically refractory TLE frequently have a very long history of seizures. In the study by Concha et al the patients had a mean duration of epilepsy of 26 years [108] whereas the patients assessed by Thivard et al have had TLE for a mean of 21 years [35]. Both of these studies found reduced FA in cingulate or temporal lobe white matter structures. In our cohort of children with TLE, the mean duration of TLE was five years and our finding of bilaterally preserved FA may reflect this shorter duration.

A third possible explanation may be variations in the response to seizures at different ages due to different susceptibility of the white matter to seizure induced injury. A decrease in FA has been suggested to indicate structural changes, such as degradation of both axonal membranes and myelin [136-138], abnormalities of myelin [139, 140] or reduced density of myelinated axons [141]. The lack of FA changes in white matter in children with TLE may suggest that the diffusion abnormalities identified in our study reflect primarily functional changes. Medically refractory TLE may affect both neuronal function, by inducing hyperexcitability, and structure, causing progressive hippocampal atrophy [5, 142]. The diffusion abnormalities seen in TLE patients could be due to a combination of functional and structural changes, where the functional changes evolve with time to

become structural. Longitudinal studies to assess alterations in the diffusion properties would be needed to confirm this this hypothesis.

One possible limitation in Study III is that differences in slice thickness of the DTI examinations between patients and controls, may affect diffusivity and/or FA. However, a recent study has found no difference in diffusivity when comparing DTI examinations with 2 and 6 mm slices, in any of the white matter structures assessed [143]. In contrast, FA was reduced on the examination performed with thicker slices in areas with crossing fibers [143], such as the superior longitudinal fasciculus. In the white matter areas that we have assessed, crossing fibers were however infrequent. Therefore it is unlikely that slice thickness would have a major effect on the findings of this study.

4.5 Clinical implications of DTI in TLE patients

Can DTI be of clinical use to lateralize seizure onset or identifying subtle lesions in TLE patients? The non-localizing nature of the diffusion abnormalities we found suggest that diffusivity or anisotropy of extratemporal white matter structures can not be used to lateralize seizure onset. Wehner et al assessed eight patients with TLE, without hippocampal sclerosis or other lesions seen on conventional imaging by DTI [144]. They found that the patients had significantly increased diffusivity (ADC) in both hippocampi compared to controls, however, as these changes were bilateral and symmetrical, DTI could not be of lateralizing value. The increased diffusivity seen in the ipsilateral hippocampus in several studies is believed to reflect disorganization due to neuronal loss, sclerosis and increased extracellular space and correlates to the finding of mesial temporal sclerosis on conventional MRI [144]. The contralateral changes are more difficult to explain but may reflect functional and/or structural effects from frequent seizure activity. Taken together, these studies suggest that at present, DTI can not reliably lateralize TLE in patients where no lesion is seen on conventional imaging.

DTI can detect regions of reduced FA and/or increased diffusivity beyond the margins of a lesion seen on conventional MRI in both adults and children with focal epilepsy [105, 126, 145]. In Study III, locally reduced FA may have occurred adjacent to the three lesions but been missed by our VOI-based analysis. To assess local changes in diffusion properties in the white matter adjacent to lesions, a ROI-based or a voxel-based approach may be more sensitive. If the regions with changes in FA and/or diffusivity adjacent to lesions are epileptogenic, they should be included in the extent of surgical resection. Studies combining DTI and MEG or invasive EEG monitoring could clarify the relationship between alterations in diffusion properties and neurophysiological data.

4.6 Optimizing tractography in epilepsy surgery candidates

Preoperative tractography to visualize the anatomical position of major white matter tracts, such as the corticospinal tract or the optic radiation, has great potential to reduce postoperative deficits in epilepsy surgery candidates. However previous studies have shown that tractography may not accurately predict the size or location of pathologically changed white matter tracts, which may result in neurological injury [146]. Mikuni et al compared direct intraoperative electrical stimulation and tractography to localize the corticospinal tract, and found that the distances between the two estimations of the

location of the tract were around 1 cm [115]. There are several factors that may adversely affect the tractography results, once high-quality DTI data have been collected. These factors can be divided into two groups: patient-dependent and method-dependent factors.

4.6.1 Patient-dependent factors

Patient-dependent factors include the type of underlying condition or lesion and the anticipated risk of brain shift. The patient´s condition or lesion may affect the diffusion properties of the white matter, and thus the tractography results. In children with TLE, we found normal FA, suggesting that this condition should not negatively affect FA-based tractography. As studies in adult TLE patients have found reduced FA in several white matter tracts [35, 108, 109], FA thresholds may need to be lower in these patients to produce similar tractography results as in normal controls.
Brain shift, i.e. movement of the brain structures after craniotomy due to the escape of cerebrospinal fluid and removal of tumor, can also influence anatomical accuracy if tractography is used intraoperatively [113]. This can be corrected for by using intraoperative DTI, however this is currently only available in a few centres in the world.

Effects of low-grade tumors on adjacent white matter tracts

In children with supratentorial low-grade tumors we could demonstrate preserved structural integrity of the white matter adjacent to the tumor. Similar findings have been reported from studies of grade II and III gliomas in adults [147, 148]. This is in contrast to high-grade tumors in adults, which frequently cause increased diffusivity and reduced anisotropy in the surrounding white matter suggesting a reduced structural integrity due to edema and tumor infiltration [98, 149]. These data suggest that low-grade tumors do not affect diffusion properties, which is favorable if tractography of the tracts adjacent to the tumor is performed. Lesions containing blood products, such as cavernomas or arteriovenous malformations may also affect the diffusion properties in the adjacent white matter [117]. Therefore tractography results in patients with lesions associated with edema or hemorrhage must be interpreted with caution and postoperative DTI should be performed when edema and/or hemorrhage have resolved.

4.6.2 Methodological factors

Currently there is no standardized method to perform tractography of the optic radiation, and the available studies have used different tracking algorithms, regions of interest and parameters to define the tracking. Wakana and coworkers have described protocols to reconstruct 11 common fiber tracts using the FACT algorithm [150]. The optic radiation was however not included, possibly as the sharp bend in its anterior portion makes it more difficult to reconstruct with a high reproducibility compared to other major white matter tracts.

The optimal algorithm for preoperative tractography has yet to be defined. The energy minimization technique identifies one single seed voxel, either anatomically [116] or by functional MRI [151] and produces a large volume of voxels which may include other white matter tracts adjacent to the tract of interest. This is depicted as a color-coded map of the probability of a connection between the voxels in the tracked tract and the seed voxel. It may however be difficult to know if a neurological deficit would result if voxels

that have a 10% probability of being connected to the seed voxel are damaged at surgery. On the other hand the line propagation technique which we and others have used involves a selection process that may result in exclusion of important white matter tracts. In spite of this, the line propagation technique may be more suitable for preoperative tractography as tracts are more clearly defined and as the calculation of the algorithm is much faster than the energy minimization algorithm. More advanced algorithms are currently developed, using two or multiple tensors, which can more accurately outline white matter tracts, including their crossings, but the time needed for data processing is still very long.

The optimal methods for selecting ROI:s and tracking parameters for tractography of the optic radiation also need to be considered. The method for ROI selection used in Study II produced a good visualization of the optic radiation. The same technique has also been used in two other studies [82, 117]. In our experience, with some training, this is a reproducible technique. To follow the sharp turning of the fibers in Meyer´s loop, it is important to select a high angulation threshold in the algorithm. To confirm that voxels with a right-left orientation in the anterior temporal stem, corresponding to the most anterior part of Meyer´s loop, are included by the tractography, the color-coded FA maps in the axial and sagittal plane should be reviewed. To determine the optimal protocol for tractography of the optic radiation further studies are needed.

5. CONCLUDING REMARKS

The findings of study I, together with previous studies of occurrence of VFD after TLR, show that the risk of developing a VFD after TLR cannot be predicted from the lateral resection size. Dissections of the optic radiation have suggested that this is due to variability in the anatomy of the optic radiation. In study II, using tractography, we could confirm a considerable variability in the anterior extent of Meyer´s loop in vivo, and could demonstrate an injury to Meyer´s loop in one patient with quadrantanopia.
At present, tractography could be used in epilepsy surgery candidates to indicate the approximate position of white matter tracts rather than as an exact anatomical landmark. In patients with TLE, tractography is a promising technique to localize the anterior extent of Meyer´s loop before TLR. This may help to predict the risk of developing a VFD after TLR and ultimately reduce the risk of postoperative VFD. Before the role of tractography to map out the optic radiation in patients with TLE can be finally established, prospective studies with perimetry and DTI before and after TLR are needed. This will determine the correlation between a postoperative visual field defect and the injury seen on tractography and clarify the intersubject variability in the anatomy of the optic radiation in patients with TLE. Studies directly comparing tractography against dissections or histological tracings of white matter tracts are another important way to validate results based on tractography to white matter anatomy.

We found widespread, bilateral diffusion abnormalities in children with TLE and a similar pattern have been reported from previous studies in adults. The nature or cause of these abnormalities is not known. They may be functional and/or structural and we have raised the possibility that primarily functional changes seen in children may evolve with time to become structural. Studies directly correlating DTI findings to histopathology and/or neurophysiology or longitudinal studies using DTI may help to clarify this issue. Whether the changes are primary, reflecting a characteristic of the epileptic brain, or secondary to the seizure activity has not been established. Studies correlating seizure frequency to DTI findings and studies of diffusion properties of the contralateral side before and after TLR may help to elucidate this. Even though the clinical importance of DTI in the preoperative evaluation for epilepsy remains to be proven, DTI contributes important information on the effects of frequent seizures on the brain and on the pathophysiological processes involved in epileptogenesis.

White matter tracts surrounding low-grade tumors in children were found to have preserved structural properties, in contrast to reports from adult high-grade brain tumors. It is crucial to avoid injury to these adjacent white matter tracts to minimize postoperative neurological deficit. Tractography may be an important tool in achieving this. However, larger prospective studies correlating tractography findings before and after tumor resection with clinical outcome measures are needed before tractography can be routinely used in surgery for low-grade brain tumors.

ACKNOWLEDGEMENTS

Many individuals have contributed to this thesis. I would like to thank the following in particular:

My supervisor Bertil Rydenhag for introducing me to research and for supporting me all the way.

My co-supervisor Kristina Malmgren for sharing her expertise in epileptology research and her patients.

Lars Frisén for introducing me to tractography, and constructive discussions and criticism.

Hans Silander for encouragement.

Thomas Skoglund for friendship and discussions on research and life in general.

Göran Starck, for teaching me about MRI and DTI.

Maria Ljungberg, Susanne Ribbelin, Lars Jönsson for productive meetings, enthusiasm and for believing in me in spite of being a beginner in MRI research.

Elysa Widjaja for sharing her great knowledge of neuroimaging in epilepsy and her research projects with me.

Charles Raybaud and Paul Babyn for creating the opportunity for me to go to Toronto.

Carter O. Snead III and James T Rutka for encouragement and for generously allowing me to study their patients.

All patients and subjects, young and old, for making the studies possible.

My colleagues at the Department of Neurosurgery, Göteborg for friendship and support.

My parents for encouraging me to seek knowledge.

Josefin for sharing her life and her passion for research with me.

This work was supported by grants from the Swedish Epilepsy Society, the Göteborg Medical Society, Glaxo Smith Kline, the Sahlgrenska Academy at Göteborg University, the Göteborg Foundation of Neurology, the ‘‘De Blindas Vänner’’ foundation, and ‘‘Stiftelsen för Medicinsk Bildering till Erik Lysholms minne.’’

REFERENCES

1. Christensen, J, Vestergaard, M, Pedersen, M G, Pedersen, C B, Olsen, J and Sidenius, P. Incidence and prevalence of epilepsy in Denmark. *Epilepsy Res*, 2007. **76**(1): p. 60-5.
2. Forsgren, L. Prevalence of epilepsy in adults in northern Sweden. *Epilepsia*, 1992. **33**(3): p. 450-8.
3. Sander, J W and Shorvon, S D. Epidemiology of the epilepsies. *J Neurol Neurosurg Psychiatry*, 1996. **61**(5): p. 433-43.
4. Fisher, R S, van Emde Boas, W, Blume, W, Elger, C, Genton, P, Lee, P and Engel, J, Jr. Epileptic seizures and epilepsy: definitions proposed by the International League Against Epilepsy (ILAE) and the International Bureau for Epilepsy (IBE). *Epilepsia*, 2005. **46**(4): p. 470-2.
5. Kwan, P and Brodie, M J. Refractory epilepsy: a progressive, intractable but preventable condition? *Seizure*, 2002. **11**(2): p. 77-84.
6. Elliott, I M, Lach, L and Smith, M L. I just want to be normal: a qualitative study exploring how children and adolescents view the impact of intractable epilepsy on their quality of life. *Epilepsy Behav*, 2005. **7**(4): p. 664-78.
7. Nilsson, L, Farahmand, B Y, Persson, P G, Thiblin, I and Tomson, T. Risk factors for sudden unexpected death in epilepsy: a case-control study. *Lancet*, 1999. **353**(9156): p. 888-93.
8. Hitiris, N, Mohanraj, R, Norrie, J and Brodie, M J. Mortality in epilepsy. *Epilepsy Behav*, 2007. **10**(3): p. 363-76.
9. Simon E A, D M J, Miller J W. Surgically treatable epilepsy syndromes in adults, in *Epilepsy Surgery - Principles and Controversies*, Miller J W, S D L, Editor. 2006, Taylor & Francis Group: New York. p. 45-71.
10. Mikati, M A, Comair, Y G and Rahi, A. Normalization of quality of life three years after temporal lobectomy: a controlled study. *Epilepsia*, 2006. **47**(5): p. 928-33.
11. Basser, P J. Inferring microstructural features and the physiological state of tissues from diffusion-weighted images. *NMR Biomed*, 1995. **8**(7-8): p. 333-44.
12. Kwan, P and Brodie, M J. Early identification of refractory epilepsy. *N Engl J Med*, 2000. **342**(5): p. 314-9.
13. Berg, A T. Understanding the delay before epilepsy surgery: who develops intractable focal epilepsy and when? *CNS Spectr*, 2004. **9**(2): p. 136-44.
14. Eriksson, S, Malmgren, K, Rydenhag, B, Jonsson, L, Uvebrant, P and Nordborg, C. Surgical treatment of epilepsy--clinical, radiological and histopathological findings in 139 children and adults. *Acta Neurol Scand*, 1999. **99**(1): p. 8-15.
15. Nilsson, L, Ahlbom, A, Farahmand, B Y and Tomson, T. Mortality in a population-based cohort of epilepsy surgery patients. *Epilepsia*, 2003. **44**(4): p. 575-81.
16. ILAE. A global survey on epilepsy surgery, 1980-1990: a report by the Commission on Neurosurgery of Epilepsy, the International League Against Epilepsy. *Epilepsia*, 1997. **38**(2): p. 249-55.
17. Wieser, H G. ILAE Commission Report. Mesial temporal lobe epilepsy with hippocampal sclerosis. *Epilepsia*, 2004. **45**(6): p. 695-714.

18. Brockhaus, A and Elger, C E. Complex partial seizures of temporal lobe origin in children of different age groups. *Epilepsia*, 1995. **36**(12): p. 1173-81.
19. Cendes F, K P, Brodie M, Andermann F. The mesio-temporal lobe epilepsy syndrome, in *Epileptic syndromes in infancy, childhood and adolescence*, Roger J, B M, Dravet C, Genton P, Tassinari C A, Wolf P, Editor. 2005, John Libbey Eurotext: Montrouge. p. 555-578.
20. Wyllie, E, Chee, M, Granstrom, M L, DelGiudice, E, Estes, M, Comair, Y, Pizzi, M, Kotagal, P, Bourgeois, B and Luders, H. Temporal lobe epilepsy in early childhood. *Epilepsia*, 1993. **34**(5): p. 859-68.
21. Eriksson, S, Nordborg, C, Rydenhag, B and Malmgren, K. Parenchymal lesions in pharmacoresistant temporal lobe epilepsy:dual and multiple pathology. *Acta Neurol Scand*, 2005. **112**(3): p. 151-156.
22. Plate, K H, Wieser, H G, Yasargil, M G and Wiestler, O D. Neuropathological findings in 224 patients with temporal lobe epilepsy. *Acta Neuropathol (Berl)*, 1993. **86**(5): p. 433-8.
23. Wieser, H G, Ortega, M, Friedman, A and Yonekawa, Y. Long-term seizure outcomes following amygdalohippocampectomy. *J Neurosurg*, 2003. **98**(4): p. 751-63.
24. Kilpatrick, C, O'Brien, T, Matkovic, Z, Cook, M and Kaye, A. Preoperative evaluation for temporal lobe surgery. *J Clin Neurosci*, 2003. **10**(5): p. 535-9.
25. Liu, Z, Nagao, T, Desjardins, G C, Gloor, P and Avoli, M. Quantitative evaluation of neuronal loss in the dorsal hippocampus in rats with long-term pilocarpine seizures. *Epilepsy Res*, 1994. **17**(3): p. 237-47.
26. Lehmann, T N, Gabriel, S, Kovacs, R, Eilers, A, Kivi, A, Schulze, K, Lanksch, W R, Meencke, H J and Heinemann, U. Alterations of neuronal connectivity in area CA1 of hippocampal slices from temporal lobe epilepsy patients and from pilocarpine-treated epileptic rats. *Epilepsia*, 2000. **41 Suppl 6**: p. S190-4.
27. Babb, T L, Brown, W J, Pretorius, J, Davenport, C, Lieb, J P and Crandall, P H. Temporal lobe volumetric cell densities in temporal lobe epilepsy. *Epilepsia*, 1984. **25**(6): p. 729-40.
28. Pitkanen, A, Tuunanen, J, Kalviainen, R, Partanen, K and Salmenpera, T. Amygdala damage in experimental and human temporal lobe epilepsy. *Epilepsy Res*, 1998. **32**(1-2): p. 233-53.
29. Bronen, R A, Cheung, G, Charles, J T, Kim, J H, Spencer, D D, Spencer, S S, Sze, G and McCarthy, G. Imaging findings in hippocampal sclerosis: correlation with pathology. *AJNR Am J Neuroradiol*, 1991. **12**(5): p. 933-40.
30. Wieshmann, U C, Woermann, F G, Lemieux, L, Free, S L, Bartlett, P A, Smith, S J, Duncan, J S, Stevens, J M and Shorvon, S D. Development of hippocampal atrophy: a serial magnetic resonance imaging study in a patient who developed epilepsy after generalized status epilepticus. *Epilepsia*, 1997. **38**(11): p. 1238-41.
31. Mohamed, A, Wyllie, E, Ruggieri, P, Kotagal, P, Babb, T, Hilbig, A, Wylie, C, Ying, Z, Staugaitis, S, Najm, I, Bulacio, J, Foldvary, N, Luders, H and Bingaman, W. Temporal lobe epilepsy due to hippocampal sclerosis in pediatric candidates for epilepsy surgery. *Neurology*, 2001. **56**(12): p. 1643-9.

32. King, D, Spencer, S S, McCarthy, G, Luby, M and Spencer, D D. Bilateral hippocampal atrophy in medial temporal lobe epilepsy. *Epilepsia*, 1995. **36**(9): p. 905-10.
33. Moran, N F, Lemieux, L, Kitchen, N D, Fish, D R and Shorvon, S D. Extrahippocampal temporal lobe atrophy in temporal lobe epilepsy and mesial temporal sclerosis. *Brain*, 2001. **124**(Pt 1): p. 167-75.
34. Babb, T L. Bilateral pathological damage in temporal lobe epilepsy. *Can J Neurol Sci*, 1991. **18**(4 Suppl): p. 645-8.
35. Thivard, L, Lehericy, S, Krainik, A, Adam, C, Dormont, D, Chiras, J, Baulac, M and Dupont, S. Diffusion tensor imaging in medial temporal lobe epilepsy with hippocampal sclerosis. *Neuroimage*, 2005. **28**(3): p. 682-90.
36. Salmenpera, T M, Simister, R J, Bartlett, P, Symms, M R, Boulby, P A, Free, S L, Barker, G J and Duncan, J S. High-resolution diffusion tensor imaging of the hippocampus in temporal lobe epilepsy. *Epilepsy Res*, 2006. **71**(2-3): p. 102-6.
37. Kimiwada, T, Juhasz, C, Makki, M, Muzik, O, Chugani, D C, Asano, E and Chugani, H T. Hippocampal and thalamic diffusion abnormalities in children with temporal lobe epilepsy. *Epilepsia*, 2006. **47**(1): p. 167-75.
38. Concha, L, Beaulieu, C, Wheatley, B M and Gross, D W. Bilateral white matter diffusion changes persist after epilepsy surgery. *Epilepsia*, 2007. **48**(5): p. 931-40.
39. Haut, S R and Moshé, S L. Is Mesial Temporal Sclerosis Caused by Early Childhood Neurological Insults, in *Epilepsy Surgery Principles and Controversies*, Miller, J W and Silbergeld, D L, Editors. 2006, Taylor & Francis Group: New York. p. 71-76.
40. Pringle, C E, Blume, W T, Munoz, D G and Leung, L S. Pathogenesis of mesial temporal sclerosis. *Can J Neurol Sci*, 1993. **20**(3): p. 184-93.
41. Pitkanen, A, Nissinen, J, Nairismagi, J, Lukasiuk, K, Grohn, O H, Miettinen, R and Kauppinen, R. Progression of neuronal damage after status epilepticus and during spontaneous seizures in a rat model of temporal lobe epilepsy. *Prog Brain Res*, 2002. **135**: p. 67-83.
42. Schramm, J, Kral, T, Grunwald, T and Blumcke, I. Surgical treatment for neocortical temporal lobe epilepsy: clinical and surgical aspects and seizure outcome. *J Neurosurg*, 2001. **94**(1): p. 33-42.
43. Benifla, M, Otsubo, H, Ochi, A, Weiss, S K, Donner, E J, Shroff, M, Chuang, S, Hawkins, C, Drake, J M, Elliott, I, Smith, M L, Snead, O C, 3rd and Rutka, J T. Temporal lobe surgery for intractable epilepsy in children: an analysis of outcomes in 126 children. *Neurosurgery*, 2006. **59**(6): p. 1203-13; discussion 1213-4.
44. Raymond, A A, Cook, M J, Fish, D R and Shorvon, S D. Cortical dysgenesis in adults with epilepsy, in *Magnetic Resonance Scanning and Epilepsy*, Shorvon, S D and al, e, Editors. 1994, Plenum Press: New York.
45. Shields, W D. Defining medical intractability: the differences in children compared to adults, in *Paediatric epilepsy syndromes and their surgical treatment*, Tuxhorn, I, Holthausen, H, and Boenigk, H, Editors. 1997, John Libbey & Company Ltd: London. p. 93-98.
46. Cross, J H, Jayakar, P, Nordli, D, Delalande, O, Duchowny, M, Wieser, H G, Guerrini, R and Mathern, G W. Proposed criteria for referral and evaluation of

children for epilepsy surgery: recommendations of the Subcommission for Pediatric Epilepsy Surgery. *Epilepsia*, 2006. **47**(6): p. 952-9.
47. Polkey, C E. Surgical treatment of epilepsy in children, in *Epilepsy in children*, Wallace, S, Editor. 1996, Chapman&Hall: London. p. 561-579.
48. Schneider, S J and Insinga, S A. Miscellaneous Brain Tumors, in *Tumors of the Pediatric Central Nervous System*, Keating, R F, Goodrich, J T, and Packer, R J, Editors. 2001, Thieme Medical Publishers: New York. p. 398-414.
49. Cross, J H. Epilepsy surgery in childhood. *Epilepsia*, 2002. **43 Suppl 3**: p. 65-70.
50. Clusmann, H, Schramm, J, Kral, T, Helmstaedter, C, Ostertun, B, Fimmers, R, Haun, D and Elger, C E. Prognostic factors and outcome after different types of resection for temporal lobe epilepsy. *J Neurosurg*, 2002. **97**(5): p. 1131-41.
51. Jackson, J H. Localised convulsions from tumour of the brain. *Brain*, 1882. **5**: p. 364-374.
52. Horsley, S. Brain-Surgery. *Br Med J*, 1886. **2**: p. 670-675.
53. Penfield, H F. Surgical therapy for temporal lobe seizures. *Arch Neurol Psychiatry*, 1950. **64**: p. 490-500.
54. Von Oertzen, J, Urbach, H, Jungbluth, S, Kurthen, M, Reuber, M, Fernandez, G and Elger, C E. Standard magnetic resonance imaging is inadequate for patients with refractory focal epilepsy. *J Neurol Neurosurg Psychiatry*, 2002. **73**(6): p. 643-7.
55. Wiebe, S, Blume, W T, Girvin, J P and Eliasziw, M. A randomized, controlled trial of surgery for temporal-lobe epilepsy. *N Engl J Med*, 2001. **345**(5): p. 311-8.
56. Quarato, P P, Di Gennaro, G, Mascia, A, Grammaldo, L G, Meldolesi, G N, Picardi, A, Giampa, T, Falco, C, Sebastiano, F, Onorati, P, Manfredi, M, Cantore, G and Esposito, V. Temporal lobe epilepsy surgery: different surgical strategies after a non-invasive diagnostic protocol. *J Neurol Neurosurg Psychiatry*, 2005. **76**(6): p. 815-24.
57. Spencer, D D, Spencer, S S, Mattsson, R H, Williamson, P D and Novelly, R A. Access to the Posterior Medial Temporal Lobe Stuctures in the Surgical Treatment of Temporal Lobe Epilepsy. *Neurosurgery*, 1984. **15**(5): p. 667-670.
58. Yasargil, M G, Teddy, P J and Roth, P. Selective amygdalohippocampectomy: operative anatomy and surgical technique, in *Advance and Technical Standards in Neurosurgery*, Symon, L, Editor. 1985, Springer: New York. p. 93-123.
59. Wieser, H G. Selective amygdalohippocampectomy has major advantages, in *Epilepsy surgery: Controversies and Principles*, Miller, J W and Silbergeld, D L, Editors. 2006, Taylor & Francis Group: New York. p. 472-478.
60. McKhann, G M. Selective Amygdalohippocampectomy: Is Less Really Better, in *Epilepsy Surgery: Controversies and Principles*, Miller, J W and Silbergeld, D L, Editors. 2006, Taylor&Francis Group: New York. p. 479-484.
61. Clusmann, H, Kral, T, Gleissner, U, Sassen, R, Urbach, H, Blumcke, I, Bogucki, J and Schramm, J. Analysis of different types of resection for pediatric patients with temporal lobe epilepsy. *Neurosurgery*, 2004. **54**(4): p. 847-59; discussion 859-60.
62. Asztely, F, Ekstedt, G, Rydenhag, B and Malmgren, K. Long term follow-up of the first 70 operated adults in the Goteborg Epilepsy Surgery Series with respect

to seizures, psychosocial outcome and use of antiepileptic drugs. *J Neurol Neurosurg Psychiatry*, 2007. **78**(6): p. 605-9.
63. Sinclair, D B, Aronyk, K E, Snyder, T J, Wheatley, B M, McKean, J D, Bhargava, R, Hoskinson, M, Hao, C, Colmers, W F, Berg, M and Mak, W. Pediatric epilepsy surgery at the University of Alberta: 1988-2000. *Pediatr Neurol*, 2003. **29**(4): p. 302-11.
64. Tellez-Zenteno, J F, Dhar, R and Wiebe, S. Long-term seizure outcomes following epilepsy surgery: a systematic review and meta-analysis. *Brain*, 2005. **128**(Pt 5): p. 1188-98.
65. Villemure, J G and Daniel, R T. Peri-insular hemispherotomy in paediatric epilepsy. *Childs Nerv Syst*, 2006. **22**(8): p. 967-81.
66. Delalande, O, Bulteau, C, Dellatolas, G, Fohlen, M, Jalin, C, Buret, V, Viguier, D, Dorfmuller, G and Jambaque, I. Vertical parasagittal hemispherotomy: surgical procedures and clinical long-term outcomes in a population of 83 children. *Neurosurgery*, 2007. **60**(2 Suppl 1): p. ONS19-32; discussion ONS32.
67. Rougier, A, Claverie, B, Pedespan, J M, Marchal, C and Loiseau, P. Callosotomy for intractable epilepsy: overall outcome. *J Neurosurg Sci*, 1997. **41**(1): p. 51-7.
68. Rydenhag, B and Silander, H C. Complications of epilepsy surgery after 654 procedures in Sweden, September 1990-1995: a multicenter study based on the Swedish National Epilepsy Surgery Register. *Neurosurgery*, 2001. **49**(1): p. 51-6; discussion 56-7.
69. Behrens, E, Schramm, J, Zentner, J and König, R. Surgical and neurological complications in a series of 708 epilepsy surgery procedures. *Neurosurgery*, 1997. **41**(1): p. 1-10.
70. Cushing, H. The field defects produced by temporal lobe lesions. *Brain*, 1922. **44**: p. 341-396.
71. Egan, R A, Shults, W T, So, N, Burchiel, K, Kellogg, J X and Salinsky, M. Visual field deficits in conventional anterior temporal lobectomy versus amygdalohippocampectomy. *Neurology*, 2000. **55**(12): p. 1818-22.
72. Hughes, T S, Abou-Khalil, B, Lavin, P J, Fakhoury, T, Blumenkopf, B and Donahue, S P. Visual field defects after temporal lobe resection: a prospective quantitative analysis. *Neurology*, 1999. **53**(1): p. 167-72.
73. Katz, A, Awad, I A, Kong, A K, Chelune, G J, Naugle, R I, Wyllie, E, Beauchamp, G and Luders, H. Extent of resection in temporal lobectomy for epilepsy. II. Memory changes and neurologic complications. *Epilepsia*, 1989. **30**(6): p. 763-71.
74. Nilsson, D, Malmgren, K, Rydenhag, B and Frisen, L. Visual field defects after temporal lobectomy -- comparing methods and analysing resection size. *Acta Neurol Scand*, 2004. **110**(5): p. 301-7.
75. Tecoma, E, S, Laxer, K D, Barbaro, N M and Plant, G T. Frequency and characteristics of visual field deficits after surgery for mesial temporal sclerosis. *Neurology*, 1993. **43**: p. 1235-1238.
76. Jensen, I and Seedorf, H. Temporal lobe epilepsy and neuro-ophthalmology. Ophthalmological findings in 74 temporal lobe resected patients. *Acta Ophthal*, 1976. **54**: p. 827-840.

77. Marino, R, Jr. and Rasmussen, T. Visual field changes after temporal lobectomy in man. *Neurology*, 1968. **18**(9): p. 825-35.
78. Barton, J J, Hefter, R, Chang, B, Schomer, D and Drislane, F. The field defects of anterior temporal lobectomy: a quantitative reassessment of Meyer's loop. *Brain*, 2005. **128**(Pt 9): p. 2123-33.
79. Manji, H and T, P G. Epilepsy surgery, visual fields, and driving: a study of the visual field criteria for driving in patients after temporal lobe epilepsy surgery with a comparison of Goldmann and Esterman perimetry. *J Neurol Neurosurg Psychiatry*, 2000. **68**: p. 80-82.
80. Archambault, L. Le faisceau longitudinal inferieur et le faisceau optique central: Quelques considerations sur les fibres d´association du cerveau. *Rev Neurol*, 1906. **4**: p. 1206.
81. Meyer, A. The connections of the occipital lobes and the present status of the cerebral visual affections. *Trans Assoc Am Physicians*, 1907. **22**: p. 7-16.
82. Yamamoto, T, Yamada, K, Nishimura, T and Kinoshita, S. Tractography to depict three layers of visual field trajectories to the calcarine gyri. *Am J Ophthalmol*, 2005. **140**(5): p. 781-785.
83. Miller, N R and Newman, N J, *Walsh and Hoyt´s Clinical Neuro-ophthalmology*. 1998, Baltimore: Williams and Wilkins.
84. Ludwig, K, *Atlas Cerebri Humani*. 1956: Karger, Basel.
85. Burgel, U, Schormann, T, Schleicher, A and Zilles, K. Mapping of histologically identified long fiber tracts in human cerebral hemispheres to the MRI volume of a reference brain: position and spatial variability of the optic radiation. *Neuroimage*, 1999. **10**(5): p. 489-99.
86. Kier, E L, Staib, L H, Davis, L M and Bronen, R A. MR imaging of the temporal stem: anatomic dissection tractography of the uncinate fasciculus, inferior occipitofrontal fasciculus, and Meyer's loop of the optic radiation. *AJNR Am J Neuroradiol*, 2004. **25**(5): p. 677-91.
87. Kier, E L, Staib, L H, Davis, L M and Bronen, R A. Anatomic dissection tractography: a new method for precise MR localization of white matter tracts. *AJNR Am J Neuroradiol*, 2004. **25**(5): p. 670-6.
88. Beaulieu, C. The basis of anisotropic water diffusion in the nervous system - a technical review. *NMR Biomed*, 2002. **15**(7-8): p. 435-55.
89. MNI. *Mapping ICB. Average of 152 T1-weighted stereotaxic volumes from the ICBM project, http://www.bic.mni.mcgill.ca/cgi/icbm_view/.*
90. Wallis, L I, Widjaja, E, Wignall, E L, Wilkinson, I D and Griffiths, P D. Misrepresentation of surface rendering of pediatric brain malformations performed following spatial normalization. *Acta Radiol*, 2006. **47**(10): p. 1094-9.
91. Mori, S and Zhang, J. Principles of diffusion tensor imaging and its applications to basic neuroscience research. *Neuron*, 2006. **51**(5): p. 527-39.
92. Bammer, R, Acar, B and Moseley, M E. In vivo MR tractography using diffusion imaging. *Eur J Radiol*, 2003. **45**(3): p. 223-34.
93. Mori, S and van Zijl, P C. Fiber tracking: principles and strategies - a technical review. *NMR Biomed*, 2002. **15**(7-8): p. 468-80.

94. Melhem, E R, Mori, S, Mukundan, G, Kraut, M A, Pomper, M G and van Zijl, P C. Diffusion tensor MR imaging of the brain and white matter tractography. *AJR Am J Roentgenol*, 2002. **178**(1): p. 3-16.
95. Ciccarelli, O, Toosy, A T, Parker, G J, Wheeler-Kingshott, C A, Barker, G J, Miller, D H and Thompson, A J. Diffusion tractography based group mapping of major white-matter pathways in the human brain. *Neuroimage*, 2003. **19**(4): p. 1545-55.
96. Catani, M, Howard, R J, Pajevic, S and Jones, D K. Virtual in vivo interactive dissection of white matter fasciculi in the human brain. *Neuroimage*, 2002. **17**(1): p. 77-94.
97. Basser, P J and Jones, D K. Diffusion-tensor MRI: theory, experimental design and data analysis - a technical review. *NMR Biomed*, 2002. **15**(7-8): p. 456-67.
98. Field, A S, Alexander, A L, Wu, Y C, Hasan, K M, Witwer, B and Badie, B. Diffusion tensor eigenvector directional color imaging patterns in the evaluation of cerebral white matter tracts altered by tumor. *J Magn Reson Imaging*, 2004. **20**(4): p. 555-62.
99. Wakana, S, Jiang, H, Nagae-Poetscher, L M, van Zijl, P C and Mori, S. Fiber tract-based atlas of human white matter anatomy. *Radiology*, 2004. **230**(1): p. 77-87.
100. Schmahmann, J D, Pandya, D N, Wang, R, Dai, G, D'Arceuil, H E, de Crespigny, A J and Wedeen, V J. Association fibre pathways of the brain: parallel observations from diffusion spectrum imaging and autoradiography. *Brain*, 2007. **130**(Pt 3): p. 630-53.
101. Lin, C P, Tseng, W Y, Cheng, H C and Chen, J H. Validation of diffusion tensor magnetic resonance axonal fiber imaging with registered manganese-enhanced optic tracts. *Neuroimage*, 2001. **14**(5): p. 1035-47.
102. Dyrby, T B, Sogaard, L V, Parker, G J, Alexander, D C, Lind, N M, Baare, W F, Hay-Schmidt, A, Eriksen, N, Pakkenberg, B, Paulson, O B and Jelsing, J. Validation of in vitro probabilistic tractography. *Neuroimage*, 2007. **37**(4): p. 1267-1277.
103. Yogarajah, M and Duncan, J S. Diffusion-based magnetic resonance imaging and tractography in epilepsy. *Epilepsia*, 2007.
104. Rugg-Gunn, F J, Eriksson, S H, Symms, M R, Barker, G J and Duncan, J S. Diffusion tensor imaging of cryptogenic and acquired partial epilepsies. *Brain*, 2001. **124**(Pt 3): p. 627-36.
105. Eriksson, S H, Rugg-Gunn, F J, Symms, M R, Barker, G J and Duncan, J S. Diffusion tensor imaging in patients with epilepsy and malformations of cortical development. *Brain*, 2001. **124**(Pt 3): p. 617-26.
106. Thivard, L, Adam, C, Hasboun, D, Clemenceau, S, Dezamis, E, Lehericy, S, Dormont, D, Chiras, J, Baulac, M and Dupont, S. Interictal diffusion MRI in partial epilepsies explored with intracerebral electrodes. *Brain*, 2006. **129**(Pt 2): p. 375-85.
107. Bertram, E H, Zhang, D X, Mangan, P, Fountain, N and Rempe, D. Functional anatomy of limbic epilepsy: a proposal for central synchronization of a diffusely hyperexcitable network. *Epilepsy Res*, 1998. **32**(1-2): p. 194-205.

108. Concha, L, Beaulieu, C and Gross, D W. Bilateral limbic diffusion abnormalities in unilateral temporal lobe epilepsy. *Ann Neurol*, 2005. **57**(2): p. 188-96.
109. Gross, D W, Concha, L and Beaulieu, C. Extratemporal white matter abnormalities in mesial temporal lobe epilepsy demonstrated with diffusion tensor imaging. *Epilepsia*, 2006. **47**(8): p. 1360-3.
110. Yu, C S, Li, K C, Xuan, Y, Ji, X M and Qin, W. Diffusion tensor tractography in patients with cerebral tumors: a helpful technique for neurosurgical planning and postoperative assessment. *Eur J Radiol*, 2005. **56**(2): p. 197-204.
111. Nguyen, T H, Yoshida, M, Stievenart, J L, Iba-Zizen, M T, Bellinger, L, Abanou, A, Kitahara, K and Cabanis, E A. MR tractography with diffusion tensor imaging in clinical routine. *Neuroradiology*, 2005. **47**(5): p. 334-43.
112. Nimsky, C, Ganslandt, O, Hastreiter, P, Wang, R, Benner, T, Sorensen, A G and Fahlbusch, R. Preoperative and intraoperative diffusion tensor imaging-based fiber tracking in glioma surgery. *Neurosurgery*, 2005. **56**(1): p. 130-7; discussion 138.
113. Nimsky, C, Ganslandt, O, Merhof, D, Sorensen, A G and Fahlbusch, R. Intraoperative visualization of the pyramidal tract by diffusion-tensor-imaging-based fiber tracking. *Neuroimage*, 2006. **30**(4): p. 1219-29.
114. Nimsky, C, Ganslandt, O and Fahlbusch, R. Implementation of fiber tract navigation. *Neurosurgery*, 2006. **58**(4 Suppl 2): p. ONS-292-303; discussion ONS-303-4.
115. Mikuni, N, Okada, T, Enatsu, R, Miki, Y, Hanakawa, T, Urayama, S, Kikuta, K, Takahashi, J A, Nozaki, K, Fukuyama, H and Hashimoto, N. Clinical impact of integrated functional neuronavigation and subcortical electrical stimulation to preserve motor function during resection of brain tumors. *J Neurosurg*, 2007. **106**(4): p. 593-8.
116. Powell, H W, Parker, G J, Alexander, D C, Symms, M R, Boulby, P A, Wheeler-Kingshott, C A, Barker, G J, Koepp, M J and Duncan, J S. MR tractography predicts visual field defects following temporal lobe resection. *Neurology*, 2005. **65**(4): p. 596-9.
117. Kikuta, K, Takagi, Y, Nozaki, K, Hanakawa, T, Okada, T, Miki, Y, Fushimi, Y, Fukuyama, H and Hashimoto, N. Early experience with 3-T magnetic resonance tractography in the surgery of cerebral arteriovenous malformations in and around the visual pathway. *Neurosurgery*, 2006. **58**(2): p. 331-7; discussion 331-7.
118. Duvernoy, H M and Bourgouin, P, *The human hippocampus: functional anatomy, vascularization and serial sections with MRI*. 2nd completely rev. and expanded ed. 1998, Berlin; New York: Springer. viii, 213.
119. Ebeling, U and Reulen, H J. Neurosurgical topography of the optic radiation in the temporal lobe. *Acta Neurochir (Wien)*, 1988. **92**(1-4): p. 29-36.
120. Mori, S, Kaufmann, W E, Davatzikos, C, Stieltjes, B, Amodei, L, Fredericksen, K, Pearlson, G D, Melhem, E R, Solaiyappan, M, Raymond, G V, Moser, H W and van Zijl, P C. Imaging cortical association tracts in the human brain using diffusion-tensor-based axonal tracking. *Magn Reson Med*, 2002. **47**(2): p. 215-23.
121. Stieltjes, B, Kaufmann, W E, van Zijl, P C, Fredericksen, K, Pearlson, G D, Solaiyappan, M and Mori, S. Diffusion tensor imaging and axonal tracking in the human brainstem. *Neuroimage*, 2001. **14**(3): p. 723-35.

122. Niewenhuys R, V J, van Huijzen C, *The Human Central Nervous System*. 1988, Berlin: Springer-Verlag.
123. Saeki, N, Fujimoto, N, Kubota, M and Yamaura, A. MR demonstration of partial lesions of the lateral geniculate body and its functional intra-nuclear topography. *Clin Neurol Neurosurg*, 2003. **106**(1): p. 28-32.
124. Catani, M, Jones, D K, Donato, R and Ffytche, D H. Occipito-temporal connections in the human brain. *Brain*, 2003. **126**(Pt 9): p. 2093-107.
125. Jiang, H, van Zijl, P C, Kim, J, Pearlson, G D and Mori, S. DtiStudio: resource program for diffusion tensor computation and fiber bundle tracking. *Comput Methods Programs Biomed*, 2006. **81**(2): p. 106-16.
126. Widjaja, E, Blaser, S, Miller, E, Kassner, A, Shannon, P, Chuang, S H, Snead, O C, 3rd and Raybaud, C R. Evaluation of Subcortical White Matter and Deep White Matter Tracts in Malformations of Cortical Development. *Epilepsia*, 2007.
127. van den Berge, J H, Schouten, H J, Boomstra, S, van Drunen Littel, S and Braakman, R. Interobserver agreement in assessment of ocular signs in coma. *J Neurol Neurosurg Psychiatry*, 1979. **42**(12): p. 1163-8.
128. Falconer, M A and Wilson, J L. Visual field changes following temporal lobectomy: their significance in relation to "Meyer´s loop" of the optic radiation. *Brain*, 1958. **81**(1): p. 1-14.
129. Babb, T L, Wilson, C L and Crandall, P H. Asymmetry and ventral course of the human geniculostriate pathway as determined by hippocampal visual evoked potentials and subsequent visual field defects after temporal lobectomy. *Exp Brain Res*, 1982. **47**(3): p. 317-28.
130. Guenot, M, Krolak-Salmon, P, Mertens, P, Isnard, J, Ryvlin, P, Fischer, C, Vighetto, A, Mauguiere, F and Sindou, M. MRI assessment of the anatomy of optic radiations after temporal lobe epilepsy surgery. *Stereotact Funct Neurosurg*, 1999. **73**(1-4): p. 84-7.
131. Peuskens, D, van Loon, J, Van Calenbergh, F, van den Bergh, R, Goffin, J and Plets, C. Anatomy of the anterior temporal lobe and the frontotemporal region demonstrated by fiber dissection. *Neurosurgery*, 2004. **55**(5): p. 1174-84.
132. Novak K, K K, Pataraia K, Marschalek J, Reitner A, Baumgartner C, Czech T. Incidence of visual field defects following selective amygdalohippocampectomy. *Epilepsia*, 2004. **45**(Suppl 3): p. 62.
133. Sincoff, E H, Tan, Y and Abdulrauf, S I. White matter fiber dissection of the optic radiations of the temporal lobe and implications for surgical approaches to the temporal horn. *J Neurosurg*, 2004. **101**(5): p. 739-46.
134. Miyagi, Y, Shima, F, Ishido, K, Araki, T, Taniwaki, Y, Okamoto, I and Kamikaseda, K. Inferior temporal sulcus approach for amygdalohippocampectomy guided by a laser beam of stereotactic navigator. *Neurosurgery*, 2003. **52**(5): p. 1117-23; discussion 1123-4.
135. Jiang, Z L, Wang, Z C and Jiang, T. [Surgical outcomes of different approaches for mesial temporal lobe gliomas]. *Zhonghua Yi Xue Za Zhi*, 2005. **85**(34): p. 2428-32.
136. Beaulieu, C, Does, M D, Snyder, R E and Allen, P S. Changes in water diffusion due to Wallerian degeneration in peripheral nerve. *Magn Reson Med*, 1996. **36**(4): p. 627-31.

137. Pierpaoli, C, Barnett, A, Pajevic, S, Chen, R, Penix, L R, Virta, A and Basser, P. Water diffusion changes in Wallerian degeneration and their dependence on white matter architecture. *Neuroimage*, 2001. **13**(6 Pt 1): p. 1174-85.
138. Werring, D J, Brassat, D, Droogan, A G, Clark, C A, Symms, M R, Barker, G J, MacManus, D G, Thompson, A J and Miller, D H. The pathogenesis of lesions and normal-appearing white matter changes in multiple sclerosis: a serial diffusion MRI study. *Brain*, 2000. **123 (Pt 8)**: p. 1667-76.
139. Gulani, V, Webb, A G, Duncan, I D and Lauterbur, P C. Apparent diffusion tensor measurements in myelin-deficient rat spinal cords. *Magn Reson Med*, 2001. **45**(2): p. 191-5.
140. Song, S K, Sun, S W, Ramsbottom, M J, Chang, C, Russell, J and Cross, A H. Dysmyelination revealed through MRI as increased radial (but unchanged axial) diffusion of water. *Neuroimage*, 2002. **17**(3): p. 1429-36.
141. Takahashi, S, Yonezawa, H, Takahashi, J, Kudo, M, Inoue, T and Tohgi, H. Selective reduction of diffusion anisotropy in white matter of Alzheimer disease brains measured by 3.0 Tesla magnetic resonance imaging. *Neurosci Lett*, 2002. **332**(1): p. 45-8.
142. Leite, J P, Neder, L, Arisi, G M, Carlotti, C G, Jr., Assirati, J A and Moreira, J E. Plasticity, synaptic strength, and epilepsy: what can we learn from ultrastructural data? *Epilepsia*, 2005. **46 Suppl 5**: p. 134-41.
143. Oouchi, H, Yamada, K, Sakai, K, Kizu, O, Kubota, T, Ito, H and Nishimura, T. Diffusion anisotropy measurement of brain white matter is affected by voxel size: underestimation occurs in areas with crossing fibers. *AJNR Am J Neuroradiol*, 2007. **28**(6): p. 1102-6.
144. Wehner, T, Lapresto, E, Tkach, J, Liu, P, Bingaman, W, Prayson, R A, Ruggieri, P and Diehl, B. The value of interictal diffusion-weighted imaging in lateralizing temporal lobe epilepsy. *Neurology*, 2007. **68**(2): p. 122-7.
145. Dumas de la Roque, A, Oppenheim, C, Chassoux, F, Rodrigo, S, Beuvon, F, Daumas-Duport, C, Devaux, B and Meder, J F. Diffusion tensor imaging of partial intractable epilepsy. *Eur Radiol*, 2005. **15**(2): p. 279-85.
146. Kinoshita, M, Yamada, K, Hashimoto, N, Kato, A, Izumoto, S, Baba, T, Maruno, M, Nishimura, T and Yoshimine, T. Fiber-tracking does not accurately estimate size of fiber bundle in pathological condition: initial neurosurgical experience using neuronavigation and subcortical white matter stimulation. *Neuroimage*, 2005. **25**(2): p. 424-9.
147. Goebell, E, Paustenbach, S, Vaeterlein, O, Ding, X Q, Heese, O, Fiehler, J, Kucinski, T, Hagel, C, Westphal, M and Zeumer, H. Low-grade and anaplastic gliomas: differences in architecture evaluated with diffusion-tensor MR imaging. *Radiology*, 2006. **239**(1): p. 217-22.
148. Tropine, A, Vucurevic, G, Delani, P, Boor, S, Hopf, N, Bohl, J and Stoeter, P. Contribution of diffusion tensor imaging to delineation of gliomas and glioblastomas. *J Magn Reson Imaging*, 2004. **20**(6): p. 905-12.
149. Stadlbauer, A, Ganslandt, O, Buslei, R, Hammen, T, Gruber, S, Moser, E, Buchfelder, M, Salomonowitz, E and Nimsky, C. Gliomas: histopathologic evaluation of changes in directionality and magnitude of water diffusion at diffusion-tensor MR imaging. *Radiology*, 2006. **240**(3): p. 803-10.

150. Wakana, S, Caprihan, A, Panzenboeck, M M, Fallon, J H, Perry, M, Gollub, R L, Hua, K, Zhang, J, Jiang, H, Dubey, P, Blitz, A, van Zijl, P and Mori, S. Reproducibility of quantitative tractography methods applied to cerebral white matter. *Neuroimage*, 2007. **36**(3): p. 630-44.
151. Toosy, A T, Ciccarelli, O, Parker, G J, Wheeler-Kingshott, C A, Miller, D H and Thompson, A J. Characterizing function-structure relationships in the human visual system with functional MRI and diffusion tensor imaging. *Neuroimage*, 2004. **21**(4): p. 1452-63.